

Source-field approach to phase-matched cascade correlated emissionP. R. Berman  and A. Kuzmich*Department of Physics, University of Michigan, Ann Arbor, Michigan 48109-1040, USA* (Received 8 August 2023; accepted 20 November 2023; published 21 December 2023)

A theory of phase-matched cascade correlated emission is developed based on a source field approach. An ensemble of three-level atoms is prepared in a phased state for which the probability to have two excitations is negligibly small. The field intensity radiated on each of the transitions is calculated. The radiation on the upper transition is isotropic and unpolarized, but the phase-matched component on the lower transition can be directional and polarized. Moreover, for sufficiently high optical densities, the emission on the lower transition can be superradiant. In addition to the field intensities, the joint probability for emission on both transitions is calculated, exhibiting correlations in both the directions of emission and polarization of the fields.

DOI: [10.1103/PhysRevA.108.063713](https://doi.org/10.1103/PhysRevA.108.063713)**I. INTRODUCTION**

Cascade emission from a single atom or from an ensemble of atoms is a fundamental process encountered in atomic physics. For a “three-level” atom prepared in its highest excited state, the vacuum radiation field induces a cascade emission to its lower levels. Kimble, Mezzacappa, and Milonni (KMM) [1] review the literature related to single-atom cascade emission and point out its importance in experiments used to test Bell’s inequalities. They also note that the central idea behind some calculations of correlated emission on the two transitions involves the assumption that the observation of a photon emitted on the upper transition projects the system into a state from which the subsequent emission occurs. One goal of their paper was to show that the same conclusions could be reached more formally using source-field theory. Subsequently, quantum state trajectory methods [2] were used to analyze this problem. In their paper, KMM focused on the time evolution of the radiated signals and did not allow for magnetic state degeneracy of the levels involved in the transitions. In contrast, theories of polarization correlation in cascade emission such as those used to analyze experiments that test Bell’s inequalities [3], must properly account for the magnetic state structure of the levels.

Over the past two decades, cascade systems have taken on increased importance owing to their relevance in quantum information protocols. In a typical scenario [4], radiation fields are used to create a two-photon coherence between levels 1 and 3 in the three-level scheme depicted in Fig. 1. One can then apply a readout field on the 3-2 transition to produce collectively enhanced phase-matched emission on the 2-1 transition. The same level scheme can be used *without* a readout pulse to produce phase-matched, correlated photon pairs [5]. Attractive features of this approach include high rate generation of narrow-bandwidth photonic entanglement of near-infrared (~ 780 nm or ~ 850 nm) and telecom (~ 1.35 μ m and ~ 1.35 μ m) fields. The former are suitable for mapping into quantum memories while the latter may be used for long-distance transmission over optical fibers. Thus, photon

pair generation using the cascade level scheme is naturally suited for applications in scalable quantum networks. In a state trajectory theory of such correlated emission [6] it is customary to assert that observation of the first photon projects the ensemble into a collective state. This collective state, in turn, emits superradiant, phase-matched emission on the 1-2 transition, provided the optical density of the atomic ensemble is much greater than unity. Other theoretical approaches involve the use of stochastic differential equations [7] and biphoton probability distributions [8].

In this paper, we extend the source-field theory of KMM to the case of phase-matched emission from an ensemble of three-level atoms that have been prepared in a spatially correlated superposition of levels 1 and 3 with a negligibly small probability to have two excitations in the ensemble. Such an initial state can be approximated by using weak excitation fields. Alternatively a mechanism such as the dipole blockade [9] can be used to excite a single collective Rydberg excitation in the ensemble, followed by a transfer of this state to a single collective excitation of level 3. Levels 1 and 3 have total angular momentum $J = 0$, while level 2 has total angular momentum $J = 1$. As such we take into account effects arising from the magnetic state degeneracy of level 2. Subsequent emission from the initial state consists of two components. First, there is “normal” spontaneous decay that depends only on the level-3 populations of the atoms created by the excitation fields. The polarizations of the emitted photons are correlated, but there is no enhanced phase-matched emission for this component. Second, and of relevance to the present discussion, there can be phase-matched, correlated two-photon emission that depends on the 1-3 coherence created by the excitation fields. The emission of the radiation on the lower transition is strongly correlated with the emission on the upper transition when phase matching is achieved. Moreover, the emission on the lower transition can be collectively enhanced for large optical densities. The polarization and spatial distribution of the radiation emitted on the lower transition can depend critically on whether the initial state is prepared by co- or counterpropagating laser fields.

In general this problem poses considerable theoretical challenges. The central problem that must be addressed is how excitation is transferred from a sublevel of level 2 in a given atom to a sublevel of level 2 in all the other atoms. In the simplest approach to this problem, all interactions between the atoms are neglected, as are propagation effects. This low density limit is the one normally considered in optical coherent transients [10]. One can arrive at expressions for correlated phase-matched emission, but the theory is problematic for two, connected reasons. The low density assumption rules out any superradiant emission on the 2-1 transition. Moreover the calculation in this optical coherent transient limit leads to a total energy radiated by the sample that is greater than the energy originally stored in the atomic ensemble [11]. To include superradiant effects for higher density samples, the next simplest approach is that taken by Rehler and Eberly (RE) [12]. They assume that each atom in the ensemble decays at the same rate, and use that assumption plus energy conservation to calculate the decay rate. This produces qualitatively correct results, but results that, nevertheless, cannot be totally correct since the calculation neglects propagation effects. In other words, as the phase-matched emission leaves the sample it is clear that atoms at different points in the sample cannot decay at the same rate. The RE model actually corresponds to the second type of superradiance discussed by Dicke [13] in his seminal paper, that resulting from phase-matched emission from a sample that is prepared with spatial phase coherence. This is distinct from the first type of superradiance discussed by Dicke in which the atoms are initially in a totally inverted state.

A fully rigorous treatment of this problem would account for all dipole-dipole interactions between an atom in a sublevel of level 2 with other atoms in their ground states. For two, two-level atoms, the role of excitation exchange of this nature has been studied by numerous authors, starting with the papers of Stephen [14] and Hutchinson and Hamerka [15]. A complete description of the radiation pattern of the two atoms was given by Lehmberg [16], although he did not include any effects related to magnetic state degeneracy. Attempts to generalize the two-atom result for a single excitation in an ensemble of N two-level atoms were developed by Svindinsky *et al.* [17] and by Friedberg and Manassah [18]. These theories were based on numerical solutions of the coupled differential equations for an ensemble of N atoms (for which the numerical calculations become increasingly time intensive with increasing N) and on the use of a continuum approximation for the atomic density. The role of magnetic degeneracy on phase-matched emission from an atomic array was considered by Miroshnychenko *et al.* [19], but the upper transition was driven by a classical laser field in the problem they considered. We are not aware of other studies of the role of excitation exchange in cascade systems that include effects arising from magnetic state degeneracy, aside from state trajectory models that, in effect, employ an approximation of the RE type [6]. The combination of the source-field approach with the RE approximation that we adopt in this paper leads to relatively simple analytic results for the quantities of physical interest, even if the RE model has its limitations.

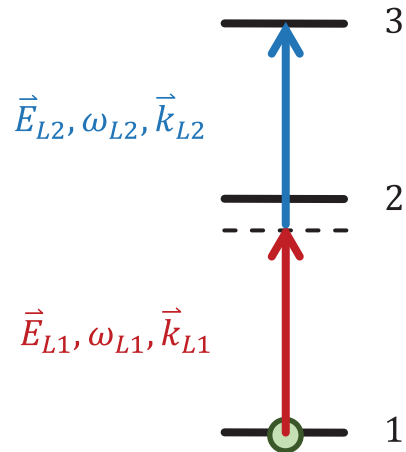


FIG. 1. Atomic energy level diagram of each atom in the ensemble. Levels 1 and 3 have total angular momentum $J = 0$, while level 2 has total angular momentum $J = 1$. Pulsed laser fields create a coherence between levels 1 and 3. The fields can be co- or counter-propagating. In the case of counterpropagating fields, it is assumed that $k_{L1} \approx k_{L2} \approx k_{21} \approx k_{32} = \omega_{32}/c$.

II. GENERAL CONSIDERATIONS

The level scheme of each atom is shown in Fig. 1. To simplify the calculation without sacrificing the relevant physics, we assume that levels 1 and 3 have total angular momentum $J = 0$, while level 2 has total angular momentum $J = 1$. It is fairly straightforward to generalize the calculation to arbitrary angular momenta. The frequency separation between levels 2 and 1 is denoted by ω_{21} and that between levels 3 and 2 by ω_{32} . There are two detectors located at positions \mathbf{D}_A and \mathbf{D}_B , both of which are in the radiation zone of the fields emitted by the atoms.

Each atom is assumed to have been prepared in a superposition of levels 1 and 3. We consider two initial state vectors for the ensemble. The first is a factorized state of the atoms that is prepared using two weak, coherent state fields having frequencies $\omega_{L1} = k_{L1}c$ and $\omega_{L2} = k_{L2}c$, giving rise to an initial state vector

$$\begin{aligned}
 |\psi(0)\rangle &= \prod_{j=1}^N (\alpha|1\rangle_j + \beta e^{i\mathbf{k}\cdot\mathbf{R}_j}|3\rangle_j) \\
 &\approx |111 \dots 111\rangle + \beta \sum_{j=-1}^N e^{i\mathbf{k}\cdot\mathbf{R}_j} |111 \dots 3_j \dots 111\rangle,
 \end{aligned} \tag{1}$$

where $\mathbf{\kappa} = \mathbf{k}_{L1} + \mathbf{k}_{L2}$, \mathbf{R}_j is the position of atom j , $|111 \dots 3_j \dots 111\rangle$ is the state in which atom j is in state 3 and all the other atoms are in their ground state, α and β are state amplitudes, and it has been assumed that $N|\beta|^2 \ll 1$, where N is the number of atoms in the ensemble. The second initial state we consider is the single-phased-excitation state

$$|\psi(0)\rangle = \frac{1}{\sqrt{N}} \sum_{j=-1}^N e^{i\mathbf{k}\cdot\mathbf{R}_j} |111 \dots 3_j \dots 111\rangle. \tag{2}$$

The nonvanishing initial state density matrix elements are

$$\begin{aligned}\rho_{11}^{(j)}(0) &= |\alpha|^2 \approx 1, \quad \rho_{33}^{(j)}(0) = |\beta|^2, \\ \rho_{31}^{(j)}(0) &= [\rho_{13}^{(j)}(0)]^* = \beta e^{i\mathbf{k}\cdot\mathbf{R}_j}\end{aligned}\quad (3)$$

for the factorized state and

$$\rho_{33}^{(j)}(0) = 1/N, \quad \rho_{31}^{(j)}(0) = [\rho_{13}^{(j)}(0)]^* = (1/\sqrt{N})e^{i\mathbf{k}\cdot\mathbf{R}_j} \quad (4)$$

for the single phased excitation state.

To calculate the intensity recorded at the detectors we need to obtain an expression for the source field operator associated with emission from the ensemble of atoms. A general expression for the positive frequency component of the source field operator is given in Appendix A. For the level scheme of Fig. 1 this expression reduces to

$$\begin{aligned}\mathbf{E}_s^+(\mathbf{R}, t) &= \left(\frac{\omega_{21}^2 \langle 2\|\mu\|3 \rangle}{4\pi\epsilon_0 c^2 R} \right) e^{i(k_{21}R - \omega_{21}t)} \\ &\times \sum_{m=-1}^1 \sum_{j=1}^N \mathbf{Q}_{1m} e^{-i\mathbf{k}_{21}\cdot\mathbf{R}_j} \sigma_{1m}^{(j)}(t_r) \\ &+ \left(\frac{\omega_{32}^2 \langle 1\|\mu\|2 \rangle}{4\pi\epsilon_0 c^2 R} \right) e^{i(k_{32}R - \omega_{32}t)} \\ &\times \sum_{m=-1}^1 \sum_{j=1}^N e^{-i\mathbf{k}_{32}\cdot\mathbf{R}_j} \mathbf{Q}_{m3} \sigma_{m3}^{(j)}(t_r),\end{aligned}\quad (5)$$

where

$$\mathbf{Q}_{1m}(\theta, \phi) = \frac{1}{\sqrt{6}} \begin{Bmatrix} \delta_{m,1}(-i\hat{\mathbf{u}}_\phi + \cos\theta\hat{\mathbf{u}}_\theta)e^{-i\phi} \\ +\delta_{m,-1}(-i\hat{\mathbf{u}}_\phi - \cos\theta\hat{\mathbf{u}}_\theta)e^{i\phi} \\ +\sqrt{2}\delta_{m,0}\sin\theta\hat{\mathbf{u}}_\theta \end{Bmatrix}, \quad (6)$$

$$\mathbf{Q}_{m3}(\theta, \phi) = \frac{1}{\sqrt{6}} \begin{Bmatrix} \delta_{m,-1}(-i\hat{\mathbf{u}}_\phi + \cos\theta\hat{\mathbf{u}}_\theta)e^{-i\phi} \\ +\delta_{m,1}(-i\hat{\mathbf{u}}_\phi - \cos\theta\hat{\mathbf{u}}_\theta)e^{i\phi} \\ -\sqrt{2}\delta_{m,0}\sin\theta\hat{\mathbf{u}}_\theta \end{Bmatrix}, \quad (7)$$

$\langle G\|\mu\|H \rangle$ is a reduced matrix element of the dipole operator between levels G and H , $t_r = t - R/c$ is a retarded time,

$$\mathbf{k}_{32} = (\omega_{32}/c)(\mathbf{R}/R), \quad \mathbf{k}_{21} = (\omega_{21}/c)(\mathbf{R}/R), \quad (8)$$

$\hat{\mathbf{u}}_\theta$ and $\hat{\mathbf{u}}_\phi$ are unit vectors, θ and ϕ are polar coordinates, and $\sigma_{1m}^{(j)}$ is a lowering operator between state $|2m\rangle$ and state $|1\rangle$ in atom j , while $\sigma_{m3}^{(j)}$ is a lowering operator between state $|3\rangle$ and state $|2m\rangle$ in atom j . All atomic and field operators are written in an interaction representation. It has been assumed that $\gamma L/c \ll 1$, where γ is a characteristic decay rate and L a characteristic dimension of the sample. In effect, retardation is neglected *within* the sample.

We can use the equation for the field operator to obtain formal expressions for quantities of physical interest. Let us assume that detector A records only emission on the 3-2 transition and detector B only emission on the 2-1 transition. Moreover, let us further assume that $D_A = D_B = D$, implying that the probability to obtain a photocount at detector A at time t and a photocount at detector B at time $t + \tau$ is nonvanishing only for $\tau > 0$. We denote the spherical coordinates of detector q by (D_q, θ_q, ϕ_q) ($q = A, B$). Then the intensity of the $\lambda_\alpha^{(q)}$

polarization component ($\alpha = \theta, \phi$) of the field per unit solid angle at detector D_q at time t is given by

$$I_\alpha(\Omega_q; t) = 2\epsilon_0 c D^2 \langle E_s^-(\mathbf{D}_q, t; \lambda_\alpha^{(q)}) E_s^+(\mathbf{D}_q, t; \lambda_\alpha^{(q)}) \rangle, \quad (9)$$

where $E_s^+(\mathbf{D}_q, t; \lambda_1^{(q)})$ is the $\hat{\mathbf{u}}_\theta$ component of $\mathbf{E}_s^+(\mathbf{D}_q, t)$, $E_s^+(\mathbf{D}_q, t; \lambda_2^{(q)})$ is the $\hat{\mathbf{u}}_\phi$ component of $\mathbf{E}_s^+(\mathbf{D}_q, t)$ and $E_s^- = (E_s^+)^{\dagger}$, and $\Omega_q = (\theta_q, \phi_q)$ denotes the spherical angles of detector q . We shall also need to find the joint probability to detect a photon having polarization $\lambda_\alpha^{(A)}$ at time t at detector A and a photon having polarization $\lambda_{\alpha'}^{(B)}$ at time $t + \tau$ at detector B , which is proportional to the function

$$\begin{aligned}g_{\alpha, \alpha'}(\Omega_A, \Omega_B; t, \tau) \\ = (2\epsilon_0 c D^2)^2 \left\langle \begin{array}{l} E_s^-(\mathbf{D}_A, t; \lambda_\alpha^{(A)}) E_s^-(\mathbf{D}_B, t + \tau; \lambda_{\alpha'}^{(B)}) \\ E_s^+(\mathbf{D}_B, t + \tau; \lambda_{\alpha'}^{(B)}) E_s^+(\mathbf{D}_A, t; \lambda_\alpha^{(A)}) \end{array} \right\rangle.\end{aligned}\quad (10)$$

The field operators in Eqs. (9) and (10) are related by Eq. (5) and its adjoint to the atomic lowering and raising operators of the individual atoms. In general, Eqs. (9) and (10) are very difficult to evaluate using Eq. (5) because the evolution operators for the atomic lowering operators appearing in Eq. (5) form a set of at least N coupled differential equations, owing to the vacuum-field-induced coupling between pairs of atoms.

To further simplify matters, we shall assume that the excitation fields are either co- or counterpropagating along the z axis,

$$\boldsymbol{\kappa} = \mathbf{k}_{L1} + \mathbf{k}_{L2} = (k_{L1} \pm k_{L2})\hat{\mathbf{z}}, \quad (11)$$

and that the fields are in two-photon resonance with the 1-3 transition,

$$\omega_{L1} + \omega_{L2} = \omega_{32} + \omega_{21} = \omega_{31}. \quad (12)$$

The fields excite an atomic density $\mathcal{N}(\mathbf{R})$ which is taken to be given by

$$\mathcal{N}(\mathbf{R}) = \frac{N}{\pi a^2 L} e^{-\rho^2/a^2} H(L) = \mathcal{N} e^{-\rho^2/a^2} H(L), \quad (13)$$

where

$$H(L) = \begin{cases} 1 & -L/2 < z < L/2 \\ 0 & \text{otherwise} \end{cases}. \quad (14)$$

$\mathcal{N} = N/(\pi a^2 L)$, and ρ is the cylindrical coordinate. The excitation scheme and atomic density distribution are meant to mirror that of typical experimental setups.

III. INTENSITIES AT BOTH DETECTORS

To treat the vacuum-induced coupling between the atoms, we adopt the simplified model that was used by Rehler and Eberly (RE) [12]. In effect we assume that each atom has the same decay dynamics. The emission on the upper transition occurs at the isolated atom decay rate,

$$\gamma_3 = \frac{\omega_{32}^3 |\langle 2\|\mu\|3 \rangle|^2}{3\pi\epsilon_0 \hbar c^3}; \quad (15)$$

there can be no collective decay on this transition since there is at most one excitation in the sample. That is, a given atom

in level 3 cannot exchange its excitation with another atom in level 2 since we have ruled out the possibility of two excitations in the ensemble. On the other hand radiation from level 2 *can* be exchanged with other ground state atoms, leading to superradiant emission. In the RE model this is accounted for by assuming that decay from level 2 occurs at a rate Γ_2 that differs from the isolated atom decay rate

$$\gamma_2 = \frac{\omega_{21}^3 |\langle 1 || \mu || 2 \rangle|^2}{9\pi\epsilon_0 \hbar c^3}. \quad (16)$$

The rate Γ_2 is chosen to guarantee energy conservation. Although interactions are not included explicitly in the RE model, they are included implicitly owing to the fact that $\Gamma_2 \neq \gamma_2$. While the RE model may not properly account for some propagation effects and can lead to some unphysical predictions, it can provide a semiquantitative approximation to the actual decay dynamics and the resulting radiation pattern.

In Appendix B, it is shown that the intensity per unit solid angle at detector A having polarization $\hat{\theta}_A$ or $\hat{\phi}_A$ is given by

$$I_{\hat{\theta}_A, \hat{\phi}_A}(\Omega_A; t) = N \frac{\hbar \omega_{32} \gamma_3}{8\pi} \rho_{33}(0), \quad (17)$$

where $\rho_{33}(0)$ is the j -independent initial upper state population of atom j . As could have been anticipated, this radiation is unpolarized and isotropic since the transition originates on a level having $J = 0$ that is (obviously) unpolarized. The total energy radiated on this transition is

$$W_A = \int_0^\infty dt \int d\Omega_A [I_{\hat{\theta}}(\Omega_A; t) + I_{\hat{\phi}}(\Omega_A; t)] = N \hbar \omega_{32} \rho_{33}(0). \quad (18)$$

This result is independent of whether the fields are co- or counterpropagating.

A. Copropagating excitation fields

For emission on the lower transition, the calculation is somewhat more involved (see Appendix B). If the fields are copropagating, then

$$\kappa = (k_{L1} + k_{L2})\hat{\mathbf{z}} = (\omega_{31}/c)\hat{\mathbf{z}} = (k_{32} + k_{21})\hat{\mathbf{z}}. \quad (19)$$

The intensity can be written as the sum of two terms, a non-phase-matched ‘‘spontaneous’’ component and a phase-matched component,

$$I_{\hat{\theta}_B, \hat{\phi}_B}(\Omega_B; t) = N \frac{\hbar \omega_{21} \gamma_2 \gamma_3}{8\pi} \frac{e^{-\Gamma_2 t_r} - e^{-\gamma_3 t_r}}{\gamma_3 - \Gamma_2} \rho_{33}(0) \Theta(t_r) \times [1 + G_{\hat{\theta}_B, \hat{\phi}_B}(\theta_B)], \quad (20)$$

where

$$\hat{\theta}_B = \cos \theta_B \cos \phi_B \hat{\mathbf{x}} + \cos \theta_B \sin \phi_B \hat{\mathbf{y}} - \sin \theta_B \hat{\mathbf{z}}, \quad (21)$$

$$\hat{\phi}_B = -\sin \phi_B \hat{\mathbf{x}} + \cos \phi_B \hat{\mathbf{y}} \quad (22)$$

are unit polarization vectors, $G_{\hat{\theta}_B, \hat{\phi}_B}(\theta_B)$ represent the phase-matched contribution, given approximately by

$$G_{\hat{\theta}_B}(\theta_B) \approx r(\theta_B) G_{\hat{\phi}_B}(\theta_B), \quad (23a)$$

where

$$G_{\hat{\phi}_B}(\theta_B) \approx \frac{3(N-1) \sin^2 [M(\theta_B)]}{4(k_{32}a)^2 [M(\theta_B)]^2}, \quad (23b)$$

$$M(\theta_B) = \frac{k_{32}L [1 - \sqrt{1 - \left(\frac{k_{21}}{k_{32}} \sin \theta_B\right)^2}] + k_{21}L(1 - \cos \theta_B)}{2}, \quad (24)$$

and

$$r(\theta_B) = \left[\cos \theta_B \sqrt{1 - \left(\frac{k_{21}}{k_{32}} \sin \theta_B\right)^2} - \frac{k_{21}}{k_{32}} \sin^2 \theta_B \right]^2. \quad (25)$$

Equations (23) provide a very good approximation to the exact results provided $k_{32}L > 10$ and $F_{32} \geq 2$, where the Fresnel number F_{32} is defined here as

$$F_{32} = \frac{2\pi a^2}{\lambda_{32}L} = \frac{k_{32}a^2}{L} = \frac{(k_{32}a)^2}{k_{32}L}, \quad (26)$$

with $\lambda_{32} = 2\pi/k_{32}$.

Equation (20) hides the fact that the spontaneous and phase-matched components actually depend on different properties of the initial state vector. The spontaneous component is proportional to the initial atomic state population $\langle \sigma_{33}^{(j)}(0) \rangle = \rho_{33}(0)$, while the phase-matched component is proportional to the 1–3 coherence $\langle \sigma_{31}^{(j)}(0) \sigma_{13}^{(j')}(0) \rangle = \rho_{33}(0) e^{i\kappa \cdot \mathbf{R}_{jj'}}$ between atoms j and j' . For our initial state vector, both quantities are proportional to $\rho_{33}(0)$, which is why the off-diagonal density matrix element $\rho_{13}(0)$ does not appear explicitly in Eq. (20).

The maximum contribution from the phase-matched component occurs for $\theta_B = 0$ [20],

$$G_{\hat{\theta}_B, \hat{\phi}_B}(0) \sim \frac{3(N-1)}{4(k_{32}a)^2} = \frac{3\mathcal{N}\lambda_{32}^2 L}{16\pi}. \quad (27)$$

For phase-matched emission, we would normally expect that $G_{\hat{\theta}_B, \hat{\phi}_B}(0, \phi_B)$ is of order N . Here we see that the contribution is reduced by $1/(k_{32}a)^2$. This reduction can be given a simple physical explanation. For phase-matched emission to occur, the first photon to be emitted must be in the forward direction. Out of all possible emission directions, the probability of emission into a solid angle that will allow for phase-matched emission is $1/(k_{32}a)^2$. As a consequence, the phase-matched emission on the lower transition is reduced by this factor.

As we move away from the phase-matched direction $\theta_B = 0$, the signal is no longer unpolarized, $G_{\hat{\theta}_B}(\theta_B) \neq G_{\hat{\phi}_B}(\theta_B)$. The ratio of the $\hat{\theta}_B$ to the $\hat{\phi}_B$ phase-matched component is $r(\theta_B)$. In Fig. 2 we plot $G_{\hat{\theta}_B}(\theta_B)/(N-1)$ and $G_{\hat{\phi}_B}(\theta_B)/(N-1)$ for $k_{32}a = 20$, $k_{21}a = 15$, $k_{32}L = 40$, $k_{21}L = 30$, $\kappa L = 70$, $F_{32} = 10$. The exact results given by Eq. (B48) of Appendix B are represented by the solid curves and the approximate solutions given by Eqs. (23) by the dashed ones, with $G_{\hat{\theta}_B}(\theta_B)/(N-1)$ lying below $G_{\hat{\phi}_B}(\theta_B)/(N-1)$.

We can integrate the intensity over time and over solid angle Ω_B to get the total energy W_B radiated by the atoms on

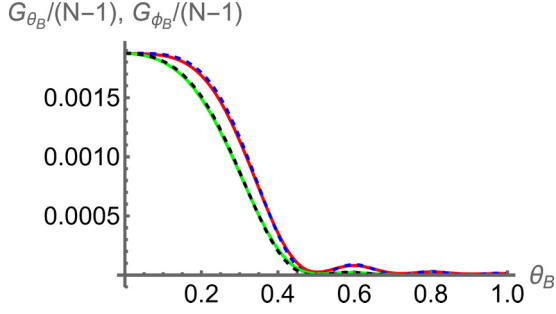


FIG. 2. Phase-matched contributions $G_{\hat{\theta}_B}(\theta_B)/(N-1)$ and $G_{\hat{\phi}_B}(\theta_B)/(N-1)$ for $k_{32}a = 20$, $k_{21}a = 15$, $k_{32}L = 40$, $k_{21}L = 30$, $\kappa L = 70$. The exact results are represented by the solid curves and the approximate solutions by the dashed ones. The curve for with $G_{\hat{\theta}_B}(\theta_B)/(N-1)$ lies below that for $G_{\hat{\phi}_B}(\theta_B)/(N-1)$.

the lower transition,

$$\begin{aligned} W_B &= \int_0^\infty dt_r \int d\Omega_B [I_{\hat{\theta}_B}(\Omega_B; t_r) + I_{\hat{\phi}_B}(\Omega_B; t_r)] \\ &= N \frac{\hbar\omega_{21}\gamma_2}{\Gamma_2} \rho_{33}(0)(1 + C_1), \end{aligned} \quad (28)$$

where

$$C_1 = \frac{1}{8\pi} \int d\Omega_B [G_{\hat{\theta}_B}(\theta_B) + G_{\hat{\phi}_B}(\theta_B)]. \quad (29)$$

Within the RE model, to conserve energy we must have

$$\Gamma_2 = \gamma_2(1 + C_1). \quad (30)$$

For $k_{32}L, k_{21}L \gg 4\pi$, the $G_{\hat{\phi}_B}(\theta_B)$ integral in Eq. (29) can be approximated as

$$\begin{aligned} \frac{1}{8\pi} \int d\Omega_B G_{\hat{\phi}_B}(\theta_B) &\approx \frac{3(N-1)}{4(k_{32}a)^2} \frac{1}{4} \int_0^\infty \theta_B d\theta_B \\ &\times \frac{\sin^2[k_{21}L(1 + k_{21}/k_{32})\theta_B^2/4]}{[k_{21}L(1 + k_{21}/k_{32})\theta_B^2/4]^2} \\ &= \frac{3\pi(N-1)}{16(k_{32}a)^2 k_{21}L(1 + k_{21}/k_{32})}. \end{aligned} \quad (31)$$

The integral involving $G_{\hat{\theta}_B}(\theta_B)$ in Eq. (29) cannot be done analytically owing to the factor $r(\theta_B)$ appearing in Eq. (23a). This factor reduces the $G_{\hat{\theta}_B}(\theta_B)$ contribution to the energy from that of the $G_{\hat{\phi}_B}(\theta_B)$ component. A very rough approximation for the reduction can be obtained by expanding

$$r(\theta_B) \sim 1 - \left(\frac{k_{21}^2}{k_{32}^2} + 2\frac{k_{21}}{k_{32}} + 1 \right) \theta_B^2 \quad (32)$$

and then replacing θ_B^2 by its average value from $\theta_B = 0$ to $\theta_B^{\max} = \sqrt{4\pi/k_{21}L(1 + k_{21}/k_{32})}$, with θ_B^{\max} chosen as the first zero of the angular distribution. In this manner we obtain

$$\begin{aligned} C_1 &\approx \frac{3\pi(N-1)}{16(k_{32}a)^2 k_{21}L(1 + k_{21}/k_{32})} \\ &\times \left[2 - \frac{4\pi}{3k_{21}L(1 + k_{21}/k_{32})} \left(\frac{k_{21}^2}{k_{32}^2} + 2\frac{k_{21}}{k_{32}} + 1 \right) \right]. \end{aligned} \quad (33)$$

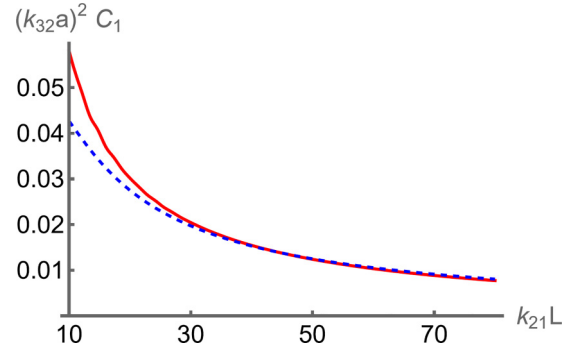


FIG. 3. Cooperativity parameter $C_1/(N-1)$ [multiplied by $(k_{32}a)^2$] for copropagating excitation as a function of kL for $ka = 20$ with $k_{21}/k_{32} = 0.75$. The solid, red curve is the exact solution, and the blue, dashed curve the approximate solution given by Eq. (33).

In Fig. 3 we plot $C_1/(N-1)$ as a function of $k_{21}L$ for $k_{32}a = 20$ with $k_{21}/k_{32} = 0.75$. The result obtained from Eq. (29) integrated over solid angle is represented by the solid curve and the approximate solution obtained using Eq. (33) by the dashed curve. As can be seen, the agreement becomes good for $k_{21}L > 30$ [21].

We see that C_1 is of order $N/[(k_{32}a)^2(k_{21}L)]$. As a consequence, $C_1 \ll 1$ if the atoms are separated, on average, by more than a wavelength, as is assumed. Even though $C_1 \ll 1$ and modifies the decay rate only slightly (and leads to a phase-matched contribution to the signal that is much less than the spontaneous component), the fact that C_1 is of order $N/[(k_{32}a)^2(k_{21}L)]$ is somewhat surprising. One might think that C_1 would be of order $N/(k_{21}k_{32}a^2)^2$ with a factor of $1/(k_{23}a)^2$ coming from the integral over Ω_A and another factor of $1/(k_{21}a)^2$ coming from the integral over Ω_B , corresponding to the small solid angle for phase-matched emission. However, this underestimates the energy. As is discussed in more detail in Appendix B, for certain *transverse* directions of phase-matched emission, there is a phase cancellation that results in an angular distribution for $G_{\hat{\theta}_B, \hat{\phi}_B}(\theta_B)$ that is governed solely by the $\sin^2[M(\theta_B)]/[M(\theta_B)]^2$ factor in Eqs. (23). The angular integration over Ω_B then leads to a factor of order $1/k_{21}L$.

B. Counterpropagating excitation fields

We now examine the corresponding result for counterpropagating field excitation with nearly equal magnitude propagation vectors, $k_{21} \approx k_{32}$, $|k_{21} - k_{32}|L \ll 1$, $|k_{21} - k_{32}|a \ll 1$, but $|\omega_{32} - \omega_{21}| \gg (\gamma_2 + \gamma_3)$. In this limit, it is possible to have phase matching, regardless of the direction of emission of the first photon. We might expect the result to be somewhat independent of θ_B ; however, this is not necessarily true in the RE model since the solid angle for phase-matched emission varies with θ_B (or θ_A).

The intensity is

$$\begin{aligned} I_{\hat{\theta}_B}^{CP}(\Omega_B; t) &= I_{\hat{\phi}_B}^{CP}(\Omega_B; t) \\ &= N \frac{\hbar\omega_{21}\gamma_2\gamma_3}{8\pi} \frac{e^{-\Gamma_2 t} - e^{-\gamma_3 t}}{\gamma_3 - \Gamma_2} \rho_{33}(0)\Theta(t_r) \\ &\times [1 + G^{CP}(\theta_B)], \end{aligned} \quad (34)$$

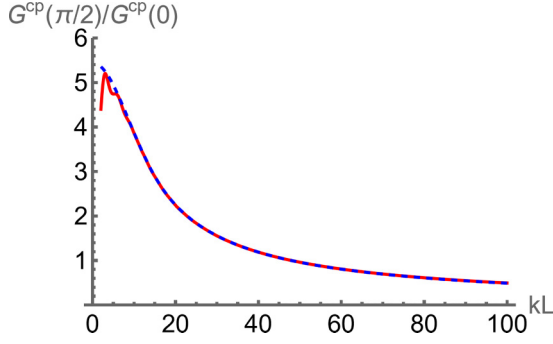


FIG. 4. Ratio $G^{cp}(\pi/2)/G^{cp}(0)$ as a function of kL for $ka = 20$. The red, solid curve is the exact result, and the dashed, blue curve is the approximate result obtained using Eq. (37).

where the phase-matched component $G^{cp}(\theta_B)$ is given approximately by (see Appendix B)

$$G^{cp}(\theta_B) \approx \frac{3(N-1)}{4ka\sqrt{2\pi}} \int_{-\infty}^{\infty} d\epsilon e^{-k^2 a^2 (\epsilon \cos \theta_B - \epsilon^2 \sin \theta_B / 2)^2 / 2} \times \frac{\sin^2 [kL\epsilon \sin(\theta_B)/2]}{(kL\epsilon \sin(\theta_B)/2)^2}. \quad (35)$$

For counterpropagating excitation, the phase-matched component is unpolarized, in contrast to that for copropagating excitation. Equation (35) provides an excellent approximation to the exact result, provided $ka > 10$, $kL > 10$, and $F_{32} \geq 1$. In the forward direction ($\theta_B = 0$) the result is unchanged from the copropagating case.

$$G_{\theta_B, \hat{\phi}_B}^{cp}(0) \approx \frac{3(N-1)}{4(ka)^2}. \quad (36)$$

A characteristic departure from this value occurs for $\theta_B = \pi/2$, where

$$G^{cp}(\pi/2) \approx \frac{3(N-1)}{4ka\sqrt{2\pi}} \int_{-\infty}^{\infty} d\epsilon e^{-k^2 a^2 \epsilon^4 / 8} \frac{\sin^2 [kL\epsilon/2]}{(kL\epsilon/2)^2}. \quad (37)$$

The ratio $G^{cp}(\pi/2)/G^{cp}(0)$ decreases with increasing kL for fixed ka . In Fig. 4 we plot $G^{cp}(\pi/2)/G^{cp}(0)$ as a function of kL for $ka = 20$. The exact result obtained from Eqs. (B47) of Appendix B (with $k_{21}a \approx k_{32}a \equiv ka$ and $\kappa L = 0$) is represented by the solid curve and the approximate solution obtained using Eq. (37) by the dashed curve. As can be seen, the approximate solution agrees with the exact solution for $kL > 10$ [21]. In Fig. 5 we plot $G^{cp}(\theta_B)/(N-1)$ as a function of θ_B for $ka = 20$ and $kL = 20$ (upper curve), 40 (middle curve), and 60 (lower curve). The exact result obtained from Eq. (B47) and the approximate solution obtained using Eq. (35) give virtually identical results for these parameters.

The total energy radiated by the atoms is still given by Eq. (28) with

$$W_B^{cp} = N \frac{\hbar \omega_{21} \gamma_2}{\Gamma_2} \rho_{33}(0) (1 + C_1^{cp}), \quad (38)$$

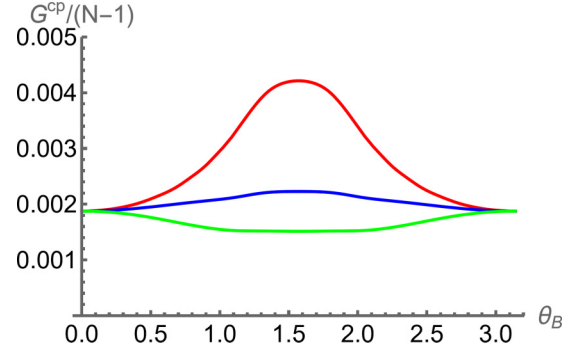


FIG. 5. Phase-matched component $G^{cp}(\theta_B)/(N-1)$ as a function of θ_B for $ka = 20$ and $kL = 20$ (red, upper curve), 40 (blue, middle curve), and 60 (green, lower curve).

where

$$C_1^{cp} = \frac{1}{4\pi} \int d\Omega_B G_{\hat{\phi}_B}^{cp}(\theta_B) = \frac{3(N-1)}{8ka\sqrt{2\pi}} \int_0^\pi \sin \theta_B d\theta_B \times \int_{-\infty}^{\infty} d\epsilon e^{-k^2 a^2 (\epsilon \cos \theta_B - \epsilon^2 \sin \theta_B / 2)^2 / 2} \times \frac{\sin^2 [kL\epsilon \sin(\theta_B)/2]}{(kL\epsilon \sin(\theta_B)/2)^2}. \quad (39)$$

Within the RE model, to conserve energy we must have

$$\Gamma_2^{cp} = \gamma_2 (1 + C_1^{cp}). \quad (40)$$

A very rough approximation for C_1^{cp} can be obtained by replacing the $\sin^2 [kL\epsilon \sin(\theta_B)/2]/(kL\epsilon \sin(\theta_B)/2)^2$ by $\sqrt{2\pi} \zeta \exp[-k^2 a^2 (\sin^2 \theta_B)/8]$, as if we had chosen a Gaussian distribution for the longitudinal component of the density. The factor ζ is an adjustable parameter of order unity. In this manner, the integral can be approximated as

$$C_1^{cp} \approx \frac{3(N-1)\sqrt{2\pi}\zeta}{8ka} \int_0^\pi \sin \theta_B d\theta_B \times \sqrt{\frac{1}{k^2 a^2 \cos^2 \theta_B + k^2 L^2 \sin^2 \theta_B / 4}} = \frac{3(N-1)\sqrt{2\pi}\zeta}{4ka} \frac{\sinh^{-1} \left(\frac{2}{kL} \sqrt{k^2 a^2 - k^2 L^2 / 4} \right)}{\sqrt{k^2 a^2 - k^2 L^2 / 4}}. \quad (41)$$

In Fig. 6 we plot $C_1^{cp}/(N-1)$ as a function of kL for $ka = 20$ with $\zeta = 0.88$. The result obtained from Eq. (41) integrated over solid angle is represented by the solid curve and the approximate solution obtained using Eq. (41) by the dashed curve. Similar agreement is found for other values of ka .

IV. JOINT PROBABILITY DISTRIBUTION

We next turn our attention to the joint probability distribution, proportional to the function $g_{\alpha, \alpha'}(\Omega_A, \Omega_B; t_r, \tau)$ given in Eq. (10). Using Eqs. (10) and (5), we find that the function

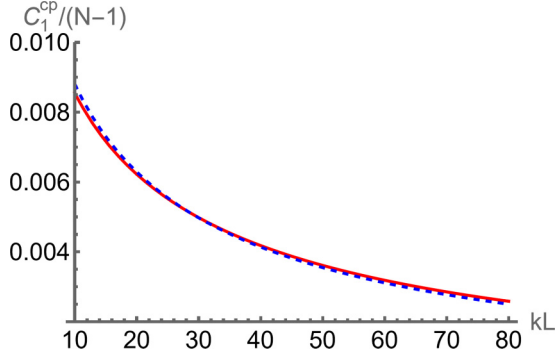


FIG. 6. Cooperativity parameter $C_1^{cp}/(N-1)$ for counterpropagating excitation as a function of kL for $ka = 20$ with $\zeta = 0.88$. The solid, red curve is the exact solution, and the blue, dashed curve the approximate solution given by Eq. (41).

$g_{\alpha,\alpha'}(\Omega_A, \Omega_B; t_r, \tau)$ depends on factors of the type

$$\sum_{j,j'=1}^N \sum_{m=-1}^1 \langle \sigma_{3m}^{(j)}(t_r) \sigma_{m'1}^{(j')}(t_r + \tau) \sigma_{1q}^{(j'')}(t_r + \tau) \sigma_{q'3}^{(j''')}(t_r) \rangle. \quad (42)$$

It is shown in Appendix B that the only nonvanishing contributions are those for which $j = j' = j'' = j'''$ and for which $(j = j', j'' = j''', j \neq j''')$. The quantum regression

$$G(\Omega_A, \Omega_B) = (N-1) \frac{\sin^2 [(\kappa - k_{32} \cos \theta_A - k_{21} \cos \theta_B)L/2]}{[(\kappa - k_{32} \cos \theta_A - k_{21} \cos \theta_B)L/2]^2} \exp \left\{ - \left[\begin{array}{l} k_{32}^2 a^2 \sin^2 \theta_A / 2 + k_{21}^2 a^2 \sin^2 \theta_B / 2 \\ + k_{32} k_{21} a^2 \sin \theta_A \sin \theta_B \cos(\phi_A - \phi_B) \end{array} \right] \right\}. \quad (46)$$

The polarizations $\Pi_{\alpha,\alpha'}(\Omega_A, \Omega_B)$ are those associated with cascade emission from a *single* isolated atom. The phase-matched contribution to the joint probability density modifies the single-atom result.

The decay rate Γ_2 is chosen so as to conserve probability,

$$\Gamma_2 = \gamma_2(1 + C_1) \quad (47)$$

with

$$C_1 = \frac{3}{(8\pi)^2} N \int d\Omega_A \int d\Omega_B \times \sum_{\alpha_A, \alpha_B} \Pi_{\alpha_A, \alpha_B}(\Omega_A, \Omega_B) G(\Omega_A, \Omega_B), \quad (48)$$

which is identical to that given in Eq. (29).

The decay rate has been chosen in a manner consistent with the RE approach. The probability to find a photon emitted on the second transition is given by

$$P_{\alpha_B}(\Omega_B, t_r) = \int_0^{t_r} dt' \int d\Omega_A P_{\alpha_A, \alpha_B}(\Omega_A, \Omega_B; t', t_r - t'), \quad (49)$$

which reproduces Eq. (20). So far so good. However, using the RE approach for this cascade emission, we run into some problems for emission on the upper transition, given by

$$P_{\alpha_A}(\Omega_A, t_r) = \int_0^\infty d\tau \int d\Omega_B P_{\alpha_A, \alpha_B}(\Omega_A, \Omega_B; t_r, \tau). \quad (50)$$

theorem [22] is then used to obtain the needed expectation values. Explicitly, we find the joint probability density $P_{\alpha_A, \alpha_B}(\Omega_A, \Omega_B; t_r, \tau)$ for a photon having polarization α_A to be detected at detector A at time t_r and a photon having polarization α_B to be detected at detector B at time $t_r + \tau$ is given by

$$P_{\alpha_A, \alpha_B}(\Omega_A, \Omega_B; t_r, \tau) = \frac{3}{(8\pi)^2} N \gamma_2 \gamma_3 e^{-\gamma_3 t_r} e^{-\Gamma_2 \tau} \tilde{P}_{\alpha_A, \alpha_B}(\Omega_A, \Omega_B), \quad (43)$$

where

$$\tilde{P}_{\alpha_A, \alpha_B}(\Omega_A, \Omega_B) = \Pi_{\alpha_A, \alpha_B}(\Omega_A, \Omega_B) [1 + G(\Omega_A, \Omega_B)], \quad (44)$$

with

$$\Pi_{\hat{\theta}_A, \hat{\theta}_B}(\Omega_A, \Omega_B) = [\cos \theta_A \cos \theta_B \cos(\phi_A - \phi_B) + \sin \theta_A \sin \theta_B]^2, \quad (45a)$$

$$\Pi_{\hat{\theta}_A, \hat{\phi}_B}(\Omega_A, \Omega_B) = \cos^2 \theta_A \sin^2(\phi_A - \phi_B), \quad (45b)$$

$$\Pi_{\hat{\phi}_A, \hat{\theta}_B}(\Omega_A, \Omega_B) = \cos^2 \theta_B \sin^2(\phi_A - \phi_B), \quad (45c)$$

$$\Pi_{\hat{\phi}_A, \hat{\phi}_B}(\Omega_A, \Omega_B) = \cos^2(\phi_A - \phi_B), \quad (45d)$$

and

Since $G(\Omega_A, \Omega_B)$ is unchanged on the exchanges $\Omega_A \leftrightarrow \Omega_B$ and $k_{21} \leftrightarrow k_{32}$, the field emitted on the upper transition is polarized in a manner similar to that on the second transition, whereas $P_{\alpha_A}(\Omega_A, t_r)$ must be isotropic and unpolarized [see Eq. (17)]. In other words, the assumption of a single decay rate for all sublevels of state 2 leads to an unphysical prediction for the polarization of the field radiated on the upper transition. A proper treatment, in which an atom in state 2 can exchange its energy with other ground-state atoms, would not lead to such inconsistencies.

A. Copropagating excitation fields

If the fields are copropagating, then $\kappa = (k_{32} + k_{21})$ and the maximum phase-matched probability occurs for $\theta_A = \theta_B = 0$, for which

$$\begin{aligned} \tilde{P}_{\hat{\theta}_A, \hat{\theta}_B}(\theta_A = \theta_B = 0, \phi_A, \phi_B) &= \tilde{P}_{\hat{\phi}_A, \hat{\phi}_B}(\theta_A = \theta_B = 0, \phi_A, \phi_B) \\ &= \cos^2(\phi_A - \phi_B) [1 + (N-1)], \end{aligned} \quad (51a)$$

$$\begin{aligned} P_{\hat{\theta}_A, \hat{\phi}_B}(\theta_A = \theta_B = 0, \phi_A, \phi_B) &= P_{\hat{\phi}_A, \hat{\theta}_B}(\theta_A = \theta_B = 0, \phi_A, \phi_B) \\ &= \sin^2(\phi_A - \phi_B) [1 + (N-1)]. \end{aligned} \quad (51b)$$

The fields are unpolarized in the forward direction [note that $\hat{\theta} = \hat{x}$ and $\hat{\theta} = \hat{y}$ in the forward direction and the $\cos^2(\phi_A - \phi_B)$ and $\sin^2(\phi_A - \phi_B)$ factors simply represent projections onto these axes]. The phase-matched component is $(N-1)$

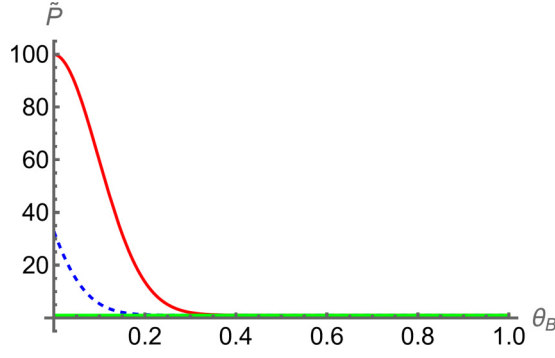


FIG. 7. Dimensionless joint probability density $\tilde{P}(\Omega_A, \Omega_B)$ as a function of θ_B for $\theta_A = 0$ (red, solid curve), 0.1 (blue, dashed curve), $\pi/2$ (green, solid line), with $k_{21}a = 10$, $k_{32}a = 15$, $k_{21}L = 20$, $k_{32}L = 30$, $N = 100$, $\phi_B = \phi_A$.

times the spontaneous component. Of course, the measured signals are calculated by averaging the field intensities over the detector areas. If the detector areas are matched to the angular width of the signals, Eqs. (51) remain valid for the measured joint probabilities. Once θ_A becomes larger $1/k_{32}a$, the phase-matched contribution to the signal becomes negligibly small, leaving only the spontaneous contribution. To illustrate this dependence, in Fig. 7 we plot $\tilde{P}(\Omega_A, \Omega_B)$ as a function of θ_B for $\theta_A = 0$ (red, solid curve), 0.1 (blue, dashed curve), $\pi/2$ (green, solid line), with $k_{21}a = 10$, $k_{32}a = 15$, $k_{21}L = 20$, $k_{32}L = 30$, $N = 100$, $\phi_B = \phi_A$. From Eq. (46), one can deduce that there can phase matching only if $\theta_A \lesssim \sqrt{2}/k_{32}a$.

B. Counterpropagating excitation fields

We now set $k_{32} = k_{21}$ and $\kappa = 0$. The maximum phase-matched probability occurs for $\theta_B = \pi - \theta_A$ and $\phi_B = \phi_A \pm \pi$. In that limit,

$$\begin{aligned} \tilde{P}_{\hat{\theta}_A, \hat{\theta}_B}^{cp}(\theta_B = \pi - \theta_A, \phi_B = \phi_A \pm \pi) \\ = \tilde{P}_{\hat{\phi}_A, \hat{\phi}_B}^{cp}(\theta_B = \pi - \theta_A, \phi_B = \phi_A \pm \pi) \\ = [1 + (N - 1)], \end{aligned} \quad (52a)$$

$$\begin{aligned} \tilde{P}_{\hat{\theta}_A, \hat{\phi}_B}(\theta_B = \pi - \theta_A, \phi_B = \phi_A \pm \pi) \\ = \tilde{P}_{\hat{\phi}_A, \hat{\theta}_B}(\theta_B = \pi - \theta_A, \phi_B = \phi_A \pm \pi) = 0. \end{aligned} \quad (52b)$$

The fields are unpolarized in the phase-matched direction, but the polarizations are correlated. In contrast to the copropagating case, phase matching now occurs for *any* θ_A , provided field B is counterpropagating relative to field A . In Fig. 8 we plot $\tilde{P}^{cp}(\Omega_A, \Omega_B)$ as a function of θ_B for $\theta_A = 0.5$ (red, solid curve), $\pi/2$ (blue, dashed curve), and 2.5 (black, dotted curve) with $k_{21}a = 10$, $k_{32}a = 15$, $k_{21}L = 20$, $k_{32}L = 30$, $N = 100$, $\phi_B = \phi_A + \pi$. As can be seen, there can now be phase matching for any θ_A .

V. DISCUSSION

We have use a source-field approach to calculate the intensity and polarizations of radiation emitted from an ensemble

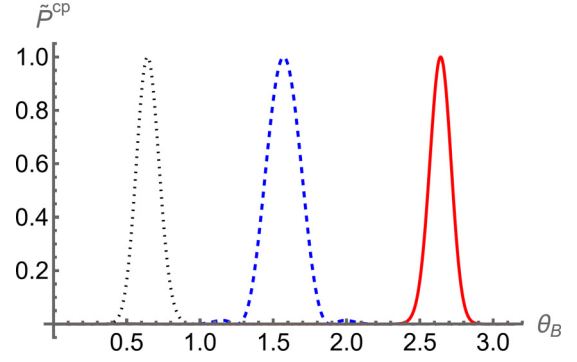


FIG. 8. Dimensionless probability density $\tilde{P}^{cp}(\Omega_A, \Omega_B)$ as a function of θ_B for $\theta_A = 0.5$ (red, solid curve), $\pi/2$ (blue, dashed curve), and 2.5 (black, dotted curve) with $k_{21}a = 10$, $k_{32}a = 15$, $k_{21}L = 20$, $k_{32}L = 30$, $N = 100$, $\phi_B = \phi_A + \pi$.

of atoms having a cascade level scheme. The atoms were prepared either in a factorized state for which the probability of having more than one excitation was negligible or in a spatially phased single excitation state. The uppermost level of each atom had angular momentum $J = 0$, the intermediate state $J = 1$, and the ground state $J = 0$. For this system, the field intensity on the upper transition is isotropic and unpolarized. The radiation emitted on the lower transition has two components, a “spontaneous” component which is unpolarized and a phase-matched component which can be polarized. Phase matching can occur if the atoms are excited using copropagating fields provided the radiation emitted on both transitions is confined to a small angular region about the direction of excitation. If counterpropagating fields are used to excite the atoms, phase matching can be achieved provided the radiation on the two transitions is emitted in opposite directions (and provided the transition frequencies are nearly equal). The joint probability distribution for both excitation schemes was also calculated.

To allow for collective emission on the lower transition, the Rehler-Eberly (RE) model was adopted, in which it is assumed that each atom decays in an identical fashion. In a source-field approach, the RE model correctly leads to the prediction that the radiation emitted on the upper transition is isotropic and unpolarized. It also gives a good semiquantitative picture of the collective enhancement of the radiation emitted on the lower transition. However, if the RE model is used to calculate the joint probability density and if that joint probability density is used to calculate the radiation emitted on the upper transition by tracing over the radiation emitted on the lower transition, the RE model leads to the incorrect prediction that the radiation emitted on the upper transition is polarized and anisotropic.

Instead of using a source-field approach, one can develop a theory based on state amplitudes. That is, as long as there is at most one excitation in the system, one can calculate the probability as $t \sim \infty$ that all the atoms are in their ground states and photons having propagation vectors \mathbf{k}_{32} and \mathbf{k}_{21} are emitted with polarizations α_A and α_B . The advantage of using this approach is that atom-atom interactions can be included exactly for fixed positions of the atoms. In such a model, energy

is always conserved and the field emitted on the upper transition is unpolarized and isotropic. Collective effects are included naturally in such a model, although one is faced with solving $3N$ coupled differential equations. If $N = 2$, one can obtain an analytic expression for the joint probability density $P_{\alpha_A, \alpha_B}(\Omega_A, \Omega_B)$ that has both spontaneous and phase-matched components. In contrast to the RE model, the integral over Ω_B now leads to unpolarized and isotropic emission on the upper transition. Moreover, it turns out that, for counterpropagating excitation and $k_{21} = k_{32}$, the radiation emitted on the lower transition is also unpolarized and isotropic, in contrast to the RE model prediction.

The amplitude approach is closely related to a state-trajectory approach that has been used to analyze phase-matched cascade emission [6]. In such an approach, the clock is started when a photocount is recorded on the upper transition, projecting the atoms into a spatially phased superposition of their ground and intermediate states. In effect, one creates a new initial state that can be used to calculate the emission on the lower transition.

If the single excitation requirement is relaxed, new physics can emerge. Suppose, for example, that *all* the atoms are excited initially. Then it is possible for the ensemble to undergo superradiant emission of the type considered by Dicke [13] for completely inverted systems. At the other extreme of a single excitation considered in this paper, we encounter the type of superradiance associated with spatial phase matching. For arbitrary initial conditions, there may be a competition between the two mechanisms.

ACKNOWLEDGMENT

This research is supported by the Air Force Office of Scientific Research and the National Science Foundation.

APPENDIX A: SOURCE-FIELD EQUATIONS

A general expression for the source field in the radiation zone resulting associated with dipole transitions from a state having angular momentum H and z component of angular momentum m_H to a lower energy state having angular momentum G and z component of angular momentum m_G is

given by [23]

$$\mathbf{E}_s^+(\mathbf{R}, t) = \left(\frac{1}{4\pi\epsilon_0 c^2 R} \right) \sum_{m_G, m_H} \sum_{\alpha, \beta=1}^3 \sum_{j=1}^N \omega_{\text{HG}}^2 \langle Gm_G | \mu_\beta | Hm_H \rangle \times [f_{\alpha\beta} - g_{\alpha\beta}(\theta, \phi)] \hat{\mathbf{u}}_\alpha \sigma_-^{(j)}(Gm_G, Hm_H; t - |\mathbf{R} - \mathbf{R}_j|/c), \quad (\text{A1})$$

where

$$f_{\alpha\beta} = (2/3)\delta_{\alpha\beta}, \quad (\text{A2a})$$

$$g_{11}(\theta, \phi) = -\frac{3\cos^2\theta - 1}{6} + \frac{\sin^2\theta \cos(2\phi)}{2}, \quad (\text{A2b})$$

$$g_{22}(\theta, \phi) = -\frac{3\cos^2\theta - 1}{6} - \frac{\sin^2\theta \cos(2\phi)}{2}, \quad (\text{A2c})$$

$$g_{33}(\theta, \phi) = \frac{3\cos^2\theta - 1}{3}, \quad (\text{A2d})$$

$$g_{12}(\theta, \phi) = g_{21} = \sin^2\theta \sin(2\phi)/2, \quad (\text{A2e})$$

$$g_{13}(\theta, \phi) = g_{31} = \sin\theta \cos\theta \cos\phi, \quad (\text{A2f})$$

$$g_{23}(\theta, \phi) = g_{32} = \sin\theta \cos\theta \sin\phi, \quad (\text{A2g})$$

$$\hat{\mathbf{u}}_1 = \hat{\mathbf{u}}_x = \sin\theta \cos\phi \hat{\mathbf{u}}_r + \cos\theta \cos\phi \hat{\mathbf{u}}_\theta - \sin\phi \hat{\mathbf{u}}_\phi, \quad (\text{A3a})$$

$$\hat{\mathbf{u}}_2 = \hat{\mathbf{u}}_y = \sin\theta \sin\phi \hat{\mathbf{u}}_r + \cos\theta \sin\phi \hat{\mathbf{u}}_\theta + \sin\phi \hat{\mathbf{u}}_\phi, \quad (\text{A3b})$$

$$\hat{\mathbf{u}}_3 = \hat{\mathbf{u}}_z = \cos\theta \hat{\mathbf{u}}_r - \sin\theta \hat{\mathbf{u}}_\theta, \quad (\text{A3c})$$

$$\mu_1 = \mu_x, \quad \mu_2 = \mu_y, \quad \mu_3 = \mu_z. \quad (\text{A4})$$

μ is the dipole moment operator, ω_{HG} is a transition frequency, $\sigma_-^{(j)}(Gm_G, Hm_H; t - |\mathbf{R} - \mathbf{R}_j|/c)$ is a lowering operator, and θ and ϕ are the polar angles of \mathbf{R} . It is assumed that the radiated field consists of components whose frequencies are close to those of the atomic transitions.

Carrying out the summation, it is possible to show that

$$\mathbf{E}_s^+(\mathbf{R}, t) = \left(\frac{1}{4\pi\epsilon_0 c^2 R} \right) \sum_{Gm_G, Hm_H} \sum_{j=1}^N \omega_{\text{HG}}^2 \mathbf{Q}(Gm_G, Hm_H) \times \sigma_-^{(j)}(Gm_G, Hm_H; t - |\mathbf{R} - \mathbf{R}_j|/c). \quad (\text{A5})$$

where

$$\mathbf{Q}(Gm_G, Hm_H) = \frac{\langle G || \mu || H \rangle}{\sqrt{2(1+2G)}} \left\{ \begin{array}{l} \left[\begin{array}{ccc} J_H & 1 & J_G \\ m_H & -1 & m_G \end{array} \right] (-i\hat{\mathbf{u}}_\phi + \cos\theta \hat{\mathbf{u}}_\theta) e^{-i\phi} \\ + \left[\begin{array}{ccc} J_H & 1 & J_G \\ m_H & 1 & m_G \end{array} \right] (-i\hat{\mathbf{u}}_\phi - \cos\theta \hat{\mathbf{u}}_\theta) e^{i\phi} \\ - \sqrt{2} \left[\begin{array}{ccc} J_H & 1 & J_G \\ m_H & 0 & m_G \end{array} \right] \sin\theta \hat{\mathbf{u}}_\theta \end{array} \right\}, \quad (\text{A6})$$

$\langle G || \mu || H \rangle$ is a reduced matrix element, and the square brackets are Clebsch-Gordan coefficients.

In the radiation zone we can write the lowering operators in an interaction representation as

$$\sigma_-^{(j)}(Gm_G, Hm_H; t - |\mathbf{R} - \mathbf{R}_j|/c) = \sigma_-^{(j)I}(Gm_G, Hm_H; t - |\mathbf{R} - \mathbf{R}_j|/c) e^{i(k_{\text{HG}}R - \omega_{\text{HG}}t)} e^{-i\mathbf{k}_{\text{HG}} \cdot \mathbf{R}_j}, \quad (\text{A7})$$

where $\mathbf{k}_{\text{HG}} = \omega_{\text{HG}}\mathbf{R}/(cR)$. Thus

$$\mathbf{E}_s^+(\mathbf{R}, t) = \left(\frac{1}{4\pi\epsilon_0 c^2 R} \right) \sum_{Gm_G, Hm_H} \sum_{j=1}^N \omega_{\text{HG}}^2 \mathbf{Q}(GJ_G m_G, HJ_H m_H) e^{i(k_{\text{HG}}R - \omega_{\text{HG}}t)} e^{-i\mathbf{k}_{\text{HG}} \cdot \mathbf{R}_j} \sigma_-^{(j)I}(GJ_G m_G, HJ_H m_H; t - |\mathbf{R} - \mathbf{R}_j|/c). \quad (\text{A8})$$

For our specific level scheme of Fig. 1 and with the neglect of retardation across the atomic ensemble, the field operator is given by Eq. (5) with $\mathbf{Q}_{m_3} \equiv \mathbf{Q}(21m, 300)$, $\mathbf{Q}_{1m} \equiv \mathbf{Q}(100, 21m)$, $\sigma_{1m}^{(j)}(t) \equiv \sigma_-^{(j)I}(100, 21m; t)$, and $\sigma_{m_3}^{(j)}(t) \equiv \sigma_-^{(j)I}(21m, 300; t)$.

APPENDIX B: CALCULATION DETAILS

In an interaction representation, the Hamiltonian for the atom-vacuum field interaction for our $J = 0 - 1 - 0$ three-level system is

$$H(t) = -i \left(\frac{\hbar\omega_{32}}{2\epsilon_0 V} \right)^{1/2} \sum_{\mathbf{k}, \lambda} \sum_{j=1}^N \sum_{m=-1}^1 \boldsymbol{\mu}_{3m} \cdot \boldsymbol{\epsilon}_{\mathbf{k}}^{(\lambda)} \sigma_{3m}^{(j)}(t) a_{\mathbf{k}, \lambda}(t) e^{i\mathbf{k} \cdot \mathbf{R}_j} e^{-i(\omega_{\mathbf{k}} - \omega_{32})t} - i \left(\frac{\hbar\omega_{21}}{2\epsilon_0 V} \right)^{1/2} \sum_{\mathbf{k}, \lambda} \sum_{j=1}^N \sum_{m=-1}^1 \boldsymbol{\mu}_{m1} \cdot \boldsymbol{\epsilon}_{\mathbf{k}}^{(\lambda)} \sigma_{m1}^{(j)}(t) a_{\mathbf{k}, \lambda}(t) \times e^{i\mathbf{k} \cdot \mathbf{R}_j} e^{-i(\omega_{\mathbf{k}} - \omega_{21})t} + \text{adjoint}, \quad (\text{B1})$$

where

$$\boldsymbol{\epsilon}_{\mathbf{k}}^{(\theta)} = \cos \theta_{\mathbf{k}} \cos \phi_{\mathbf{k}} \hat{\mathbf{x}} + \cos \theta_{\mathbf{k}} \sin \phi_{\mathbf{k}} \hat{\mathbf{y}} - \sin \theta_{\mathbf{k}} \hat{\mathbf{z}}, \quad (\text{B2})$$

$$\boldsymbol{\epsilon}_{\mathbf{k}}^{(\phi)} = -\sin \phi_{\mathbf{k}} \hat{\mathbf{x}} + \cos \phi_{\mathbf{k}} \hat{\mathbf{y}}, \quad (\text{B3})$$

$$\hat{\mathbf{k}} = \sin \theta_{\mathbf{k}} \cos \phi_{\mathbf{k}} \hat{\mathbf{x}} + \sin \theta_{\mathbf{k}} \sin \phi_{\mathbf{k}} \hat{\mathbf{y}} + \cos \theta_{\mathbf{k}} \hat{\mathbf{z}}, \quad (\text{B4})$$

and we have evaluated the radiated field frequencies at the atomic transition frequencies. Starting from this Hamiltonian, and using the evolution equations for any Heisenberg operator $O(t)$,

$$\dot{O}(t) = \frac{1}{i\hbar} [O(t), H(t)], \quad (\text{B5})$$

we can obtain the evolution equations for the various expectation values that are needed in the calculation.

Within the RE model, the evolution equations for the expectation values of the atomic operators are

$$\langle \dot{\sigma}_{m_3}^{(j)}(t) \rangle = -\frac{\Gamma_2 + \gamma_3}{2} \langle \sigma_{m_3}^{(j)}(t) \rangle, \quad (\text{B6a})$$

$$\langle \dot{\sigma}_{33}^{(j)}(t) \rangle = -\gamma_3 \langle \sigma_{33}^{(j)}(t) \rangle, \quad (\text{B6b})$$

$$\langle \dot{\sigma}_{1m}^{(j)}(t) \rangle = -\frac{\Gamma_2}{2} \langle \sigma_{1m}^{(j)}(t) \rangle, \quad (\text{B6c})$$

$$\langle \dot{\sigma}_{13}^{(j)}(t) \rangle = -\frac{\gamma_3}{2} e^{-\gamma_3 t/2} \langle \sigma_{13}^{(j)}(t) \rangle, \quad (\text{B6d})$$

$$\langle \dot{\sigma}_{mm'}^{(j)}(t) \rangle = -\Gamma_2 \langle \sigma_{mm'}^{(j)}(t) \rangle + \gamma_3 \langle \sigma_{33}^{(j)}(t) \rangle. \quad (\text{B6e})$$

The quantities $\sigma_{33}^{(j)}(t)$ and $\sigma_{mm'}^{(j)}(t)$ are atomic population operators, while $\sigma_{mm'}^{(j)}(t)$ for $m \neq m'$ is an atomic Zeeman coherence operator. It has been assumed that the frequency difference $|\omega_{32} - \omega_{21}| \gg (\gamma_2 + \gamma_3)$, allowing us to ignore any transfer of electronic state coherence produced by spontaneous emission.

At time $t = 0$, the atomic state operators are

$$\sigma_{m_3}^{(j)}(0) = |2, m\rangle^{(j)} \langle 3, 0|^{(j)}, \quad (\text{B7a})$$

$$\sigma_{33}^{(j)}(0) = |3, 0\rangle^{(j)} \langle 3, 0|^{(j)}, \quad (\text{B7b})$$

$$\sigma_{1m}^{(j)}(0) = |1, 0\rangle^{(j)} \langle 2, m|^{(j)}, \quad (\text{B7c})$$

$$\sigma_{13}^{(j)}(0) = |1, 0\rangle^{(j)} \langle 3, 0|^{(j)}, \quad (\text{B7d})$$

$$\sigma_{mm'}^{(j)}(0) = |2, m\rangle^{(j)} \langle 2, m'|^{(j)}. \quad (\text{B7e})$$

It is now a relatively simple task to calculate the field intensities using Eqs. (5), (B5), (3), and (4). In doing so, one encounters factors of the type $\langle \sigma_{3m}^{(j)}(t_r) \sigma_{m'3}^{(j')}(t_r) \rangle$ or $\langle \sigma_{m1}^{(j)}(t_r) \sigma_{1m'}^{(j')}(t_r) \rangle$.

1. Field intensities

a. Upper transition. Using Eqs. (5) and (9), we find that at detector A, the intensity per unit solid angle $I_{\theta_A, \phi_A}(\Omega_A; t)$ having polarization $\hat{\theta}_A$ or $\hat{\phi}_A$ is given by

$$I_{\hat{\theta}_A, \hat{\phi}_A}(\Omega_A; t) = \frac{3\hbar\omega_{32}\gamma_3}{8\pi} \sum_{j, j'=1}^N \sum_{m, m'=-1}^1 [\mathbf{Q}_{m_3}(\theta_A, \phi_A)]_{\hat{\theta}_A, \hat{\phi}_A}^* [\mathbf{Q}_{m'3}(\theta_A, \phi_A)]_{\hat{\theta}_A, \hat{\phi}_A} \langle \sigma_{3m}^{(j)}(t_r) \sigma_{m'3}^{(j')}(t_r) \rangle \times e^{-i\mathbf{k}_{32} \cdot \mathbf{R}_{jj'}}, \quad (\text{B8})$$

where

$$\mathbf{k}_{32} = (\omega_{32}/c)(\mathbf{D}_A/D_A) = (\sin \theta_A \cos \phi_A \hat{\mathbf{x}} + \sin \theta_A \sin \phi_A \hat{\mathbf{y}} + \cos \theta_A \hat{\mathbf{z}}) \quad (\text{B9})$$

and

$$\mathbf{R}_{jj'} = \mathbf{R}_j - \mathbf{R}_{j'}. \quad (\text{B10})$$

First, we calculate

$$\frac{d}{dt} \langle [\sigma_{3m}^{(j)}(t) \sigma_{m'3}^{(j')}(t)] \rangle = \langle [\dot{\sigma}_{3m}^{(j)}(t) \sigma_{m'3}^{(j')}(t)] \rangle + \text{adjoint}(m \iff m'). \quad (\text{B11})$$

If $j = j'$, we can use the identity

$$\sigma_{pp'}^{(j)}(t) \sigma_{qq'}^{(j)}(t) = \sigma_{pq'}^{(j)}(t) \delta_{p',q}, \quad (\text{B12})$$

to obtain

$$\langle \sigma_{3m}^{(j)}(t_r) \sigma_{m'3}^{(j)}(t_r) \rangle = \langle \sigma_{33}^{(j)}(t_r) \rangle \delta_{m,m'} = \rho_{33}^{(j)}(0) e^{-\gamma_3 t_r} \delta_{m,m'}, \quad (\text{B13})$$

where

$$\rho_{33}(0) = \begin{cases} |\beta|^2 & \text{factorized state} \\ \frac{1}{N} & \text{single excitation state} \end{cases}. \quad (\text{B14})$$

If $j \neq j'$, one might think that

$$\langle \sigma_{pp'}^{(j)}(t) \sigma_{qq'}^{(j')}(t) \rangle = \langle \sigma_{pp'}^{(j)}(t) \rangle \langle \sigma_{qq'}^{(j')}(t) \rangle, \quad (\text{B15})$$

since the atoms decay independently, but, in general, this is need not be the case if the atoms are prepared in an entangled state. On the other hand, when $j \neq j'$,

$$\sigma_{pp'}^{(j)}(t) \sigma_{qq'}^{(j')}(t) = \sigma_{qq'}^{(j')}(t) \sigma_{pp'}^{(j)}(t). \quad (\text{B16})$$

For $j \neq j'$, we use Eq. (B5) to obtain

$$\begin{aligned} \sigma_{3m}^{(j)}(t) \dot{\sigma}_{m'3}^{(j')}(t) &= -\frac{1}{\hbar} \sum_{\mathbf{k}, \lambda} \left(\frac{\hbar \omega_{32}}{2\epsilon_0 V} \right)^{1/2} \sum_{j'=1}^N \sum_{m''=-1}^1 \boldsymbol{\mu}_{3m''} \cdot \boldsymbol{\epsilon}_{\mathbf{k}}^{(\lambda)} \sigma_{3m}^{(j)}(t) [\sigma_{m'm''}^{(j')}(t) - \sigma_{33}^{(j')}(t) \delta_{m',m''}] a_{\mathbf{k}_\lambda}(t) e^{i\mathbf{k} \cdot \mathbf{R}_{j'}} e^{-i(\omega_{\mathbf{k}} - \omega_{32})t} \\ &\quad - \frac{1}{\hbar} \sum_{\mathbf{k}, \lambda} \left(\frac{\hbar \omega_{\mathbf{k}}}{2\epsilon_0 V} \right)^{1/2} \sum_{j'=1}^N [\boldsymbol{\mu}_{m'1} \cdot \boldsymbol{\epsilon}_{\mathbf{k}}^{(\lambda)}]^* a_{\mathbf{k}_\lambda}^\dagger(t) \sigma_{3m}^{(j)}(t) \sigma_{13}^{(j')}(t) e^{i\mathbf{k} \cdot \mathbf{R}_{j'}} e^{-i(\omega_{\mathbf{k}} - \omega_{21})t}, \end{aligned} \quad (\text{B17})$$

which is written in normal order form. From Eqs. (B1) and (B5), it follows that

$$\begin{aligned} \dot{a}_{\mathbf{k}_\lambda}(t) &= \frac{1}{\hbar} \left(\frac{\hbar \omega_{32}}{2\epsilon_0 V} \right)^{1/2} \sum_{j'=1}^N \sum_{m''=-1}^1 [\boldsymbol{\mu}_{3m''} \cdot \boldsymbol{\epsilon}_{\mathbf{k}}^{(\lambda)}]^* \sigma_{m''3}^{(j')}(t) e^{-i\mathbf{k} \cdot \mathbf{R}_{j'}} e^{i(\omega_{\mathbf{k}} - \omega_{32})t} + \frac{1}{\hbar} \left(\frac{\hbar \omega_{21}}{2\epsilon_0 V} \right)^{1/2} \sum_{j''=1}^N \sum_{m'''=-1}^1 [\boldsymbol{\mu}_{m''1} \cdot \boldsymbol{\epsilon}_{\mathbf{k}}^{(\lambda)}]^* \sigma_{1m''}^{(j'')}(t) \\ &\quad \times e^{-i\mathbf{k} \cdot \mathbf{R}_{j''}} e^{i(\omega_{\mathbf{k}} - \omega_{21})t}. \end{aligned} \quad (\text{B18})$$

We now use the standard approach [23] of formally integrating Eq. (B18),

$$\begin{aligned} a_{\mathbf{k}_\lambda}(t) &= a_{\mathbf{k}_\lambda}(0) + \frac{1}{\hbar} \left(\frac{\hbar \omega_{\mathbf{k}}}{2\epsilon_0 V} \right)^{1/2} \sum_{j''=1}^N \sum_{m'''=-1}^1 [\boldsymbol{\mu}_{3m'''} \cdot \boldsymbol{\epsilon}_{\mathbf{k}}^{(\lambda)}]^* \int_0^t dt' \sigma_{m'''3}^{(j'')}(t') e^{-i\mathbf{k} \cdot \mathbf{R}_{j''}} e^{i(\omega_{\mathbf{k}} - \omega_{32})t'} \\ &\quad + \frac{1}{\hbar} \left(\frac{\hbar \omega_{\mathbf{k}}}{2\epsilon_0 V} \right)^{1/2} \sum_{j''=1}^N \sum_{m'''=-1}^1 [\boldsymbol{\mu}_{m''1} \cdot \boldsymbol{\epsilon}_{\mathbf{k}}^{(\lambda)}]^* \int_0^t dt' \sigma_{1m''}^{(j'')}(t') e^{-i\mathbf{k} \cdot \mathbf{R}_{j''}} e^{i(\omega_{\mathbf{k}} - \omega_{21})t'}, \end{aligned} \quad (\text{B19})$$

and substituting it back into Eq. (B17). Since Eq. (B17) is normal ordered, all terms containing $a_{\mathbf{k}_\lambda}(0)$ and $a_{\mathbf{k}_\lambda}^\dagger(0)$ will vanish when expectation values are taken. When the summation over $\{\mathbf{k}, \lambda\}$ in Eq. (B17) is carried out, there will be contributions to $\dot{\sigma}_{m'3}^{(j')}(t)$ from atoms having $j'' \neq j'$; however since we are neglecting atom-atom interactions, we keep only those terms with $j'' = j'$. The summation over \mathbf{k} is converted to an integral over \mathbf{k} , which, in turn, leads to a delta function $\delta(t - t')$, so the atomic operators are all evaluated at the same time and we can use Eqs. (B12) and (B16). In this manner,

$$\langle \sigma_{3m}^{(j)}(t) \dot{\sigma}_{m'3}^{(j')}(t) \rangle = -\frac{(\gamma_3 + \Gamma_2)}{2} \langle \sigma_{3m}^{(j)}(t) \sigma_{m'3}^{(j')}(t) \rangle. \quad (\text{B20})$$

As a consequence, for arbitrary j and j' , we obtain

$$\frac{d}{dt} \langle \sigma_{3m}^{(j)}(t) \sigma_{m'3}^{(j')}(t) \rangle = -\gamma_3 \langle \sigma_{33}^{(j)}(t) \rangle \delta_{m,m'} \delta_{j,j'} - (\gamma_3 + \Gamma_2) \langle \sigma_{3m}^{(j)}(t) \sigma_{m'3}^{(j')}(t) \rangle (1 - \delta_{j,j'}), \quad (\text{B21})$$

having solution

$$\langle \sigma_{3m}^{(j)}(t) \sigma_{m'3}^{(j')}(t) \rangle = \langle \sigma_{33}^{(j)}(0) \rangle e^{-\gamma_3 t} \delta_{m,m'} \delta_{j,j'} + \langle \sigma_{3m}^{(j)}(0) \sigma_{m'3}^{(j')}(0) \rangle e^{-(\gamma_3 + \Gamma_2)t} (1 - \delta_{j,j'}). \quad (\text{B22})$$

For the initial states given in Eqs. (1) or (2), this reduces to

$$\langle \sigma_{3m}^{(j)}(t) \sigma_{m'3}^{(j')}(t) \rangle = \rho_{33}^{(j)}(0) e^{-\gamma_3 t} \delta_{m,m'} \delta_{j,j'}. \quad (\text{B23})$$

The Kronecker delta $\delta_{j,j'}$ is present since we have allowed for at most one excitation in our initial state.

When Eq. (B23) is substituted into Eq. (B8), the expression for the field intensity reduces to

$$I_{\hat{\theta}_A, \hat{\phi}_A}(\Omega_A; t) = \frac{3\hbar\omega_{32}\gamma_3}{8\pi} \rho_{33}^{(j)}(0) e^{-\gamma_3 t} \sum_{m, m'=-1}^1 [\mathbf{Q}_{m3}(\theta_A, \phi_A)]_{\hat{\theta}_A, \hat{\phi}_A}^* [\mathbf{Q}_{m3}(\theta_A, \phi_A)]_{\hat{\theta}_A, \hat{\phi}_A}. \quad (\text{B24})$$

Using the identity

$$\sum_{m=-1}^1 [\mathbf{Q}_{m3}(\theta_A, \phi_A)]_{\hat{\theta}_A, \hat{\phi}_A}^* [\mathbf{Q}_{m3}(\theta_A, \phi_A)]_{\hat{\theta}_A, \hat{\phi}_A} = \sum_{m=-1}^1 [\mathbf{Q}_{1m}(\theta_B, \phi_B)]_{\hat{\theta}_B, \hat{\phi}_B}^* [\mathbf{Q}_{1m}(\theta_B, \phi_B)]_{\hat{\theta}_B, \hat{\phi}_B} = \frac{1}{3}, \quad (\text{B25})$$

we arrive at Eq. (17). This result is independent of whether or not the excitation fields are co- or counterpropagating. In contrast the emission on the lower transition is different for co- or counterpropagating excitation fields.

a. Lower transition

For emission on the lower transition, the calculation is somewhat more involved. The intensity at detector B , calculated from Eqs. (9), (5), and (16), is given by

$$I_{\hat{\theta}_B, \hat{\phi}_B}(\Omega_B; t) = \frac{9\hbar\omega_{21}\gamma_2}{8\pi} \sum_{j, j'=1}^N \sum_{m, m'=-1}^1 [\mathbf{Q}_{1m}(\theta_B, \phi_B)]_{\hat{\theta}_B, \hat{\phi}_B}^* [\mathbf{Q}_{m'1}(\theta_B, \phi_B)]_{\hat{\theta}_B, \hat{\phi}_B} \langle \sigma_{m1}^{(j)}(t_r) \sigma_{m'1}^{(j')}(t_r) \rangle e^{-i\mathbf{k}_{21} \cdot \mathbf{R}_{jj'}}, \quad (\text{B26})$$

where

$$\mathbf{k}_{21} = (\omega_{21}/c)(\mathbf{D}_B/D_B)(\sin\theta_B \cos\phi_B \hat{\mathbf{x}} + \sin\theta_B \sin\phi_B \hat{\mathbf{y}} + \cos\theta_B \hat{\mathbf{z}}). \quad (\text{B27})$$

The differential equation for $\langle \sigma_{m1}^{(j)}(t) \sigma_{m'1}^{(j')}(t) \rangle$ is

$$\frac{d}{dt} \langle \sigma_{m1}^{(j)}(t) \sigma_{m'1}^{(j')}(t) \rangle = \langle \sigma_{m1}^{(j)}(t) \dot{\sigma}_{m'1}^{(j')}(t) \rangle + \text{adjoint}(m \iff m'). \quad (\text{B28})$$

Following the same procedure we find used to find $\sigma_{3m}^{(j)}(t) \dot{\sigma}_{m'3}^{(j')}(t)$, we obtain

$$\begin{aligned} \sigma_{m1}^{(j)}(t) \dot{\sigma}_{m'1}^{(j')}(t) &= -\frac{1}{\hbar} \sum_{\mathbf{k}, \lambda} \left(\frac{\hbar\omega_{\mathbf{k}}}{2\epsilon_0 V} \right)^{1/2} \sum_{j'=1}^N \sum_{m''=-1}^1 \boldsymbol{\mu}_{3m''} \cdot \boldsymbol{\epsilon}_{\mathbf{k}}^{(\lambda)} \sigma_{2m}^{(j)}(t) [\sigma_{m'm''}^{(j')}(t) - \sigma_{33}^{(j')}(t) \delta_{m', m''}] a_{\mathbf{k}, \lambda}(t) e^{i\mathbf{k} \cdot \mathbf{R}_{j'}} e^{-i(\omega_{\mathbf{k}} - \omega_{32})t} \\ &\quad - \frac{1}{\hbar} \sum_{\mathbf{k}, \lambda} \left(\frac{\hbar\omega_{\mathbf{k}}}{2\epsilon_0 V} \right)^{1/2} \sum_{j'=1}^N [\boldsymbol{\mu}_{3m'} \cdot \boldsymbol{\epsilon}_{\mathbf{k}}^{(\lambda)}]^* a_{\mathbf{k}, \lambda}^\dagger(t) \sigma_{m1}^{(j)}(t) \sigma_{13}^{(j')}(t) e^{i\mathbf{k} \cdot \mathbf{R}_{j'}} e^{-i(\omega_{\mathbf{k}} - \omega_{21})t}. \end{aligned} \quad (\text{B29})$$

We substitute Eq. (B18) into Eq. (B29) and carry out the integral over \mathbf{k} to arrive at

$$\frac{d}{dt} \langle \sigma_{m1}^{(j)}(t) \sigma_{m'1}^{(j')}(t) \rangle = -\Gamma_2 \langle \sigma_{m1}^{(j)}(t) \sigma_{m'1}^{(j')}(t) \rangle + \gamma_{jj', mm'} \langle \sigma_{31}^{(j)}(t) \sigma_{13}^{(j')}(t) \rangle, \quad (\text{B30})$$

having solution

$$\langle \sigma_{m1}^{(j)}(t) \sigma_{m'1}^{(j')}(t) \rangle = \langle \sigma_{m1}^{(j)}(0) \sigma_{m'1}^{(j')}(0) \rangle e^{-\Gamma_2 t} + \gamma_{jj', mm'} \int_0^t dt' e^{-\Gamma_2(t-t')} \langle \sigma_{31}^{(j)}(t') \sigma_{13}^{(j')}(t') \rangle, \quad (\text{B31})$$

where

$$\gamma_{jj', mm'} = \gamma_3 \frac{9}{8\pi | \langle 2 \| \boldsymbol{\mu} \| 3 \rangle |^2} \sum_{\lambda} \int d\Omega_A [\boldsymbol{\mu}_{3m'} \cdot \boldsymbol{\epsilon}_{\mathbf{k}_{32}}^{(\lambda)}]^* [\boldsymbol{\mu}_{3m} \cdot \boldsymbol{\epsilon}_{\mathbf{k}_{32}}^{(\lambda)}] e^{-i\mathbf{k}_{32} \cdot \mathbf{R}_{jj'}}, \quad (\text{B32})$$

and $\langle \sigma_{31}^{(j)}(t) \sigma_{13}^{(j')}(t) \rangle$ satisfies the differential equation

$$\frac{d}{dt} \langle \sigma_{31}^{(j)}(t) \sigma_{13}^{(j')}(t) \rangle = -\gamma_3 \langle \sigma_{31}^{(j)}(t) \sigma_{13}^{(j')}(t) \rangle. \quad (\text{B33})$$

The second term in Eq. (B31) reflects the fact that the relative spatial phase of the 1-3 coherence between different atoms that is created by the excitation fields is transferred to level 2 via spontaneous emission. Note that $\gamma_{jj', mm'} = \gamma_3 \delta_{mm'}$. The solution of Eq. (B33) is

$$\langle \sigma_{31}^{(j)}(t) \sigma_{13}^{(j')}(t) \rangle = e^{-\gamma_3 t} \langle \sigma_{31}^{(j)}(0) \sigma_{13}^{(j')}(0) \rangle = e^{-\gamma_3 t} \rho_{33}(0) e^{i\mathbf{k} \cdot \mathbf{R}_{jj'}}. \quad (\text{B34})$$

Although $\langle \sigma_{31}^{(j)}(0) \sigma_{13}^{(j')}(0) \rangle = \rho_{33}(0) e^{i\mathbf{k} \cdot \mathbf{R}_{jj'}}$ for our choice of initial conditions, it is important to note that, when $j \neq j'$, the nonvanishing of $\langle \sigma_{31}^{(j)}(0) \sigma_{13}^{(j')}(0) \rangle$ depends on the correlation between the excited state amplitudes of different atoms. Using

Eqs. (B31), (B34), (B7), and (1)–(4), we then find

$$\langle \sigma_{m1}^{(j)}(t) \sigma_{1m'}^{(j')}(t) \rangle = \gamma_{jj';mm'} \frac{e^{-\Gamma_2 t} - e^{-\gamma_3 t}}{\gamma_3 - \Gamma_2} \rho_{33}(0) e^{i\mathbf{k} \cdot \mathbf{R}_{jj'}}, \quad (\text{B35})$$

since $\langle \sigma_{m1}^{(j)}(0) \sigma_{1m'}^{(j')}(0) \rangle = 0$.

Substituting this solution into Eq. (B26), we find that the intensity emitted on the lower transition is

$$I_{\hat{\theta}_B, \hat{\phi}_B}(\Omega_B; t) = N \frac{\hbar \omega_{21} \gamma_2 \gamma_3}{8\pi} \frac{e^{-\Gamma_2 t} - e^{-\gamma_3 t}}{\gamma_3 - \Gamma_2} \rho_{33}(0) \Theta(t_r) [1 + G_{\hat{\theta}_B, \hat{\phi}_B}(\theta_B, \phi_B)], \quad (\text{B36})$$

where

$$\begin{aligned} G_{\hat{\theta}_B, \hat{\phi}_B}(\theta_B, \phi_B) &= \frac{27}{8\pi |\langle 2 || \mu || 3 \rangle|^2} \frac{1}{N} \sum_{\substack{jj'=1 \\ j \neq j'}}^N \sum_{mm'=-1}^1 [\mathbf{Q}_{1m}(\theta_B, \phi_B)]_{\hat{\theta}_B, \hat{\phi}_B}^* [\mathbf{Q}_{m'1}(\theta_B, \phi_B)]_{\hat{\theta}_B, \hat{\phi}_B} e^{i\mathbf{k} \cdot \mathbf{R}_{jj'}} e^{-i\mathbf{k}_{21} \cdot \mathbf{R}_{jj'}} \\ &\times \sum_{\lambda} \int d\Omega_A [\boldsymbol{\mu}_{3m'} \cdot \boldsymbol{\epsilon}_{\mathbf{k}_{32}}^{(\lambda)}]^* [\boldsymbol{\mu}_{3m} \cdot \boldsymbol{\epsilon}_{\mathbf{k}_{32}}^{(\lambda)}] e^{-i\mathbf{k}_{32} \cdot \mathbf{R}_{jj'}} \\ &= \frac{9}{8\pi} \frac{1}{N} \sum_{\substack{jj'=1 \\ j \neq j'}}^N \sum_{mm'=-1}^1 [\mathbf{Q}_{1m}(\theta_B, \phi_B)]_{\hat{\theta}_B, \hat{\phi}_B}^* [\mathbf{Q}_{m'1}(\theta_B, \phi_B)]_{\hat{\theta}_B, \hat{\phi}_B} e^{i\mathbf{k} \cdot \mathbf{R}_{jj'}} e^{-i\mathbf{k}_{21} \cdot \mathbf{R}_{jj'}} \sum_{\lambda} \int d\Omega_A e^{-i\mathbf{k}_{32} \cdot \mathbf{R}_{jj'}} (\boldsymbol{\epsilon}_{\mathbf{k}_{32}}^{(\lambda)})_m [(\boldsymbol{\epsilon}_{\mathbf{k}_{32}}^{(\lambda)})_{m'}]^* \end{aligned} \quad (\text{B37})$$

and $(\boldsymbol{\epsilon}_{\mathbf{k}_{32}}^{(\lambda)})_m$ is a spherical component of the polarization vector,

$$(\boldsymbol{\epsilon}_{\mathbf{k}_{32}}^{(\theta_A)})_{\pm 1} = \mp \cos \theta_A / \sqrt{2} e^{\pm i\phi_A}, \quad (\boldsymbol{\epsilon}_{\mathbf{k}_{32}}^{(\theta_A)})_0 = -\sin \theta_A, \quad (\text{B38a})$$

$$(\boldsymbol{\epsilon}_{\mathbf{k}_{32}}^{(\phi_A)})_{\pm 1} = -ie^{\pm i\phi_A} / \sqrt{2} \quad (\boldsymbol{\epsilon}_{\mathbf{k}_{32}}^{(\phi_A)})_0 = 0. \quad (\text{B38b})$$

The sums over j and j' in Eq. (B37) are converted into spatial integrals using the prescription

$$\sum_{j=1}^N f(\mathbf{R}_j) \implies \int d\mathbf{R} \mathcal{N}(\mathbf{R}) f(\mathbf{R}), \quad (\text{B39})$$

where $\mathcal{N}(\mathbf{R})$ is the atomic density given in Eq. (13).

a. Copropagating fields. For copropagating fields, with

$$\boldsymbol{\kappa} = (k_{L1} + k_{L2})\hat{\mathbf{z}} = (\omega_{31}/c)\hat{\mathbf{z}} = (k_{32} + k_{21})\hat{\mathbf{z}}, \quad (\text{B40})$$

Eq. (B37) reduces to

$$\begin{aligned} G_{\hat{\theta}_B, \hat{\phi}_B}(\theta_B, \phi_B) &= \frac{9(N-1)}{8\pi} \sum_{mm'=-1}^1 [\mathbf{Q}_{1m}(\theta_B, \phi_B)]_{\hat{\theta}_B, \hat{\phi}_B}^* [\mathbf{Q}_{m'1}(\theta_B, \phi_B)]_{\hat{\theta}_B, \hat{\phi}_B} \sum_{\lambda} \int d\Omega_A (\boldsymbol{\epsilon}_{\mathbf{k}_{32}}^{(\lambda)})_m [(\boldsymbol{\epsilon}_{\mathbf{k}_{32}}^{(\lambda)})_{m'}]^* \\ &\times e^{-K_x^2 a^2/2} e^{-K_y^2 a^2/2} \frac{\sin^2(K_z L/2)}{(K_z L/2)^2}, \end{aligned} \quad (\text{B41})$$

where

$$\mathbf{K} = (k_{32} \sin \theta_A \cos \phi_A + k_{21} \sin \theta_B \cos \phi_B)\hat{\mathbf{x}} + (k_{32} \sin \theta_A \sin \phi_A + k_{21} \sin \theta_B \sin \phi_B)\hat{\mathbf{y}} + [k_{32}(1 - \cos \theta_A) + k_{21}(1 - \cos \theta_B)]\hat{\mathbf{z}}. \quad (\text{B42})$$

Note that

$$e^{-K_x^2 a^2/2} e^{-K_y^2 a^2/2} = e^{-k_{32}^2 a^2 \sin^2 \theta_A/2} e^{-k_{21}^2 a^2 \sin^2 \theta_B/2} e^{-k_{32} k_{21} a^2 \sin \theta_A \sin \theta_B \cos(\phi_A - \phi_B)}. \quad (\text{B43})$$

The sum in Eq. (B41) can be evaluated as

$$\begin{aligned} &\sum_{mm'=-1}^1 [\mathbf{Q}_{1m}(\theta_B, \phi_B)]_{\hat{\theta}_B}^* [\mathbf{Q}_{m'1}(\theta_B, \phi_B)]_{\hat{\theta}_B} \sum_{\lambda} (\boldsymbol{\epsilon}_{\mathbf{k}_{32}}^{(\lambda)})_m [(\boldsymbol{\epsilon}_{\mathbf{k}_{32}}^{(\lambda)})_{m'}]^* \\ &= \frac{1}{3} \left[\cos^2 \theta_B - \frac{\sin^2 \theta_A}{2} (1 - 3 \sin^2 \theta_B) \right] - \frac{1}{6} \sin^2 \theta_A \cos^2 \theta_B \cos [2(\phi_A - \phi_B)] + \frac{1}{6} \sin (2\theta_A) \sin (2\theta_B) \cos (\phi_A - \phi_B), \end{aligned}$$

$$\begin{aligned} & \sum_{mm'=-1}^1 [\mathbf{Q}_{1m}(\theta_B, \phi_B)]_{\hat{\phi}_B}^* [\mathbf{Q}_{m'1}(\theta_B, \phi_B)]_{\hat{\phi}_B} \sum_{\lambda} (\epsilon_{\mathbf{k}_{32}}^{(\lambda)})_m [(\epsilon_{\mathbf{k}_{32}}^{(\lambda)})_{m'}]^* \\ &= \frac{1}{3} \left(1 - \frac{\sin^2 \theta_A}{2} \right) + \frac{1}{6} \sin^2 \theta_A \cos [2(\phi_A - \phi_B)]. \end{aligned} \tag{B44}$$

The integral over ϕ_A in Eq. (B41) can be calculated analytically if the $e^{-a \cos(\phi_A - \phi_B)}$ in that equation is expanded as

$$e^{-a \cos(\phi_A - \phi_B)} = I_0(a) + 2 \sum_{m=1}^{\infty} I_m(a) (-1)^m \cos [m(\phi_A - \phi_B)], \tag{B45}$$

where I_m is a Bessel function of the first kind. It then follows that

$$\begin{aligned} & \int_0^{2\pi} d\phi_A \sum_{mm'=-1}^1 [\mathbf{Q}_{1m}(\theta_B, \phi_B)]_{\hat{\theta}_B}^* [\mathbf{Q}_{m'1}(\theta_B, \phi_B)]_{\hat{\theta}_B} \sum_{\lambda} (\epsilon_{\mathbf{k}_{32}}^{(\lambda)})_m [(\epsilon_{\mathbf{k}_{32}}^{(\lambda)})_{m'}]^* \\ &= \frac{2\pi}{3} \left(\cos^2 \theta_B - \frac{\sin^2 \theta_A}{2} (1 - 3 \sin^2 \theta_B) \right) I_0(k_{32}k_{21}a^2 \sin \theta_A \sin \theta_B) - \frac{\pi}{3} \sin^2 \theta_A \cos^2 \theta_B I_2(k_{32}k_{21}a^2 \sin \theta_A \sin \theta_B) \\ & \quad - \frac{\pi}{3} \sin(2\theta_A) \sin(2\theta_B) I_1(k_{32}k_{21}a^2 \sin \theta_A \sin \theta_B), \end{aligned} \tag{B46a}$$

$$\begin{aligned} & \int_0^{2\pi} d\phi_A \sum_{mm'=-1}^1 [\mathbf{Q}_{1m}(\theta_B, \phi_B)]_{\hat{\phi}_B}^* [\mathbf{Q}_{m'1}(\theta_B, \phi_B)]_{\hat{\phi}_B} \sum_{\lambda} (\epsilon_{\mathbf{k}_{32}}^{(\lambda)})_m [(\epsilon_{\mathbf{k}_{32}}^{(\lambda)})_{m'}]^* \\ &= \frac{2\pi}{3} \left(1 - \frac{\sin^2 \theta_A}{2} \right) I_0(k_{32}k_{21}a^2 \sin \theta_A \sin \theta_B) + \frac{\pi}{3} \sin^2 \theta_A I_2(k_{32}k_{21}a^2 \sin \theta_A \sin \theta_B), \end{aligned} \tag{B46b}$$

independent of ϕ_B .

We then find

$$\begin{aligned} G_{\hat{\theta}_B}(\theta_B) &= \frac{3(N-1)}{4} \int_0^{\pi} d\theta_A \sin \theta_A e^{-k_{32}^2 a^2 \sin^2 \theta_A / 2} e^{-k_{21}^2 a^2 \sin^2 \theta_B / 2} \frac{\sin^2(K_z L / 2)}{(K_z L / 2)^2} \\ & \quad \times \left\{ \left(\cos^2 \theta_B - \frac{\sin^2 \theta_A}{2} (1 - 3 \sin^2 \theta_B) \right) I_0(k_{32}k_{21}a^2 \sin \theta_A \sin \theta_B) - \frac{1}{2} \sin^2 \theta_A \cos^2 \theta_B I_2(k_{32}k_{21}a^2 \sin \theta_A \sin \theta_B) \right. \\ & \quad \left. - \frac{1}{2} \sin(2\theta_A) \sin(2\theta_B) I_1(k_{32}k_{21}a^2 \sin \theta_A \sin \theta_B) \right\}, \end{aligned} \tag{B47a}$$

$$\begin{aligned} G_{\hat{\phi}_B}(\theta_B) &= \frac{3(N-1)}{4} \int_0^{\pi} d\theta_A \sin \theta_A e^{-k_{32}^2 a^2 \sin^2 \theta_A / 2} e^{-k_{21}^2 a^2 \sin^2 \theta_B / 2} \frac{\sin^2(K_z L / 2)}{(K_z L / 2)^2} \left\{ \left(1 - \frac{\sin^2 \theta_A}{2} \right) I_0(k_{32}k_{21}a^2 \sin \theta_A \sin \theta_B) \right. \\ & \quad \left. + \frac{1}{2} \sin^2 \theta_A I_2(k_{32}k_{21}a^2 \sin \theta_A \sin \theta_B) \right\}. \end{aligned} \tag{B47b}$$

To get good approximations to these equations, let us assume that $k_{32}k_{21}a^2 \sin \theta_A \sin \theta_B \gg 1$, allowing us to use the asymptotic form for the Bessel functions, $I_\nu(z) \sim e^z / \sqrt{2\pi z}$. In this limit

$$G_{\hat{\theta}_B}(\theta_B) \approx \frac{3(N-1)}{4} \int_0^{\pi} d\theta_A \sqrt{\sin \theta_A} \frac{e^{-(k_{32} \sin \theta_A - k_{21} \sin \theta_B)^2 a^2 / 2}}{\sqrt{2\pi k_{32}k_{21}a^2 \sin \theta_B}} \cos^2(\theta_A + \theta_B) \frac{\sin^2 \{ [k_{32}(1 - \cos \theta_A) + k_{21}(1 - \cos \theta_B)]L/2 \}}{\{ [k_{32}(1 - \cos \theta_A) + k_{21}(1 - \cos \theta_B)] \}^2}, \tag{B48a}$$

$$G_{\hat{\phi}_B}(\theta_B) \approx \frac{3(N-1)}{4} \int_0^{\pi} d\theta_A \sqrt{\sin \theta_A} e^{-(k_{32} \sin \theta_A - k_{21} \sin \theta_B)^2 a^2 / 2} \frac{\sin^2 \{ [k_{32}(1 - \cos \theta_A) + k_{21}(1 - \cos \theta_B)]L/2 \}}{\{ [k_{32}(1 - \cos \theta_A) + k_{21}(1 - \cos \theta_B)]L/2 \}^2}. \tag{B48b}$$

If $k_{32}a \gg 1$ the integrand is sharply peaked at $\theta_A = \sin^{-1}(k_{21} \sin \theta_B / k_{32})$, provided that $k_{21} \sin \theta_B / k_{32} < 1$, and the Fresnel number, defined in Eq. (26), is greater than one. [There is also a peak near $\theta_A = \pi - \sin^{-1}(k_{21} \sin \theta_B / k_{32})$, but this is killed

by the other factors provided $k_{32}L \gg 1$, as we assume.] In those limits, we can approximate Eqs. (B48) as

$$G_{\hat{\theta}_B}(\theta_B) \approx \frac{3(N-1)}{4k_{32}a\sqrt{2\pi}} \frac{\sin^2 [M(\theta_B)]^2}{[M(\theta_B)]^2} \left(\cos \theta_B \sqrt{1 - \left(\frac{k_{21}}{k_{32}} \sin \theta_B\right)^2} - \frac{k_{21}}{k_{32}} \sin^2 \theta_B \right) \int_0^\pi d\theta_A e^{-(k_{32} \sin \theta_A - k_{21} \sin \theta_B)^2 a^2 / 2}, \quad (\text{B49a})$$

$$G_{\hat{\phi}_B}(\theta_B) \approx \frac{3(N-1)}{4k_{32}a\sqrt{2\pi}} \frac{\sin^2 [M(\theta_B)]}{[M(\theta_B)]^2} \int_0^\pi d\theta_A e^{-(k_{32} \sin \theta_A - k_{21} \sin \theta_B)^2 a^2 / 2}, \quad (\text{B49b})$$

where

$$M_\theta(\theta_B) = \frac{k_{32}L \left[1 - \sqrt{1 - \left(\frac{k_{21}}{k_{32}} \sin \theta_B\right)^2} \right] + k_{21}L(1 - \cos \theta_B)}{2}. \quad (\text{B50})$$

By setting $\theta_A = \sin^{-1}(k_{21} \sin \theta_B / k_{32}) - \epsilon$ in Eqs. (B49) and extending the resulting integral over ϵ from $-\infty$ to ∞ , we obtain a value of $\sqrt{2\pi}/ka$ for the integral, leading to Eqs. (23).

In the forward direction, $\theta_B = 0$, we can use Eqs. (B47) to obtain

$$G_{\hat{\theta}_B, \hat{\phi}_B}(0) = \frac{3(N-1)}{4} \int_0^\pi \sin \theta_A d\theta_A e^{-k_{32}^2 a^2 \sin^2 \theta_A / 2} \frac{\sin^2 [k_{32}L \sin^2(\theta_A/2)]}{[k_{32}L \sin^2(\theta_A/2)]^2} \left(1 - \frac{\sin^2 \theta_A}{2} \right). \quad (\text{B51})$$

The signal is unpolarized in the phase-matched direction. If $k_{32}a \gg 1$ the major contribution to the integral over θ_A comes from $\theta_A \ll 1$. (There is also a contribution near $\theta_A = \pi$, but this is killed by the $\sin^2 [k_{32}L \sin^2(\theta_A/2)] / [k_{32}L \sin^2(\theta_A/2)]^2$ factor provided $k_{32}L \gg 1$, as we assume) and we can approximate $G_{\hat{\theta}_B, \hat{\phi}_B}(0)$ by

$$\begin{aligned} G_{\hat{\theta}_B, \hat{\phi}_B}(0) &\approx \frac{3(N-1)}{4} \int_0^\infty \theta_A e^{-k_{32}^2 a^2 \theta_A^2 / 2} \frac{\sin^2 [k_{32}L \theta_A^2 / 4]}{[k_{32}L \theta_A^2 / 4]^2} d\theta_A \\ &= \frac{3(N-1)}{4(k_{32}a)^2} \left\{ F_{32} \left[2 \tan^{-1}(1/F_{32}) - F_{32} \ln \left(1 + \frac{1}{F_{32}^2} \right) \right] \right\}. \end{aligned} \quad (\text{B52})$$

This expression is valid if $k_{32}L \gtrsim 10$ and $k_{32}a \gtrsim 1$. It gives the wrong value as $k_{32}L \sim 0$ ($F_{32} \sim \infty$), since the contribution to the integral near $\theta_A = \pi$ makes an equal contribution in this limit; that is, as $F_{32} \sim \infty$, the exact result given by Eq. (B51) is twice that given by Eq. (B52).

b. Counterpropagating fields. We now set $k_{21} \approx k_{32}$, $|k_{21} - k_{32}|L \ll 1$, $|k_{21} - k_{32}|a \ll 1$, but $|\omega_{32} - \omega_{21}| \gg (\gamma_2 + \gamma_3)$. In this limit, we can take over all the previous results simply by setting $k_{21}a \approx k_{32}a \equiv ka$ and replacing $\kappa L = k_{21}L + k_{32}L \approx 0$ in Eqs. (B47). As before, we expand the Bessel functions using their asymptotic forms to obtain

$$G_{\hat{\theta}_B}^{cp}(\theta_B) \approx \frac{3(N-1)}{4ka\sqrt{2\pi}} \int_0^\pi d\theta_A \sqrt{\frac{\sin \theta_A}{\sin \theta_B}} e^{-k^2 a^2 (\sin \theta_A - \sin \theta_B)^2 / 2} \cos^2(\theta_A + \theta_B) \frac{\sin^2 [kL(\cos \theta_A + \cos \theta_B)/2]}{(k(\cos \theta_A + \cos \theta_B)L/2)^2}, \quad (\text{B53a})$$

$$G_{\hat{\phi}_B}^{cp}(\theta_B) \approx \frac{3(N-1)}{4ka\sqrt{2\pi}} \int_0^\pi d\theta_A \sqrt{\frac{\sin \theta_A}{\sin \theta_B}} e^{-k^2 a^2 (\sin \theta_A - \sin \theta_B)^2 / 2} \frac{\sin^2 [kL(\cos \theta_A + \cos \theta_B)/2]}{[kL(\cos \theta_A + \cos \theta_B)/2]^2}. \quad (\text{B53b})$$

It is not difficult to show that $G_{\hat{\theta}_B, \hat{\phi}_B}^{cp}(0)$ is still given by Eq. (B52), but the major contribution to the integral occurs for $\theta_A \approx \pi$ instead of $\theta_A \approx 0$.

The integrands in Eqs. (35) are sharply peaked at $\theta_A = \pi - \theta_B$, provided $\tan \theta_B \gg 1/(2kL)$ and $\sin \theta_B \gg 1/(ka)$. In this limit the most of the factors in the integrands can be evaluated at $\theta_A = \pi - \theta_B$. Setting $\theta_A = \pi - \theta_B - \epsilon$, we can approximate Eqs. (35) by

$$G_{\hat{\theta}_B, \hat{\phi}_B}^{cp}(\theta_B) \approx \frac{3(N-1)}{4ka\sqrt{2\pi}} \int_{-\infty}^\infty d\epsilon e^{-k^2 a^2 (\epsilon \cos \theta_B - \epsilon^2 \sin \theta_B / 2)^2 / 2} \frac{\sin^2 [kL\epsilon \sin(\theta_B)/2]}{[kL\epsilon \sin(\theta_B)/2]^2}. \quad (\text{B54})$$

The phase-matched contribution of the intensity is unpolarized, in contrast to the copropagating case. Equation (B54) provides an excellent approximation to the exact result, provided $ka > 10$, $kL > 10$, and $F_{32} \geq 1$.

2. Joint probability density

The joint probability distribution $P_{\alpha_A, \alpha_B}(\Omega_A, \Omega_B; t_r, \tau)$ is proportional to the function $g_{\alpha, \alpha'}(\Omega_A, \Omega_B; t_r, \tau)$ given in Eq. (10). As long as $\tau > 0$, negligibly small errors are introduced if we neglect the field creation and annihilation operators at time $t = 0$

in evaluating $g_{\alpha,\alpha'}(\Omega_A, \Omega_B; t_r, \tau)$ [1]. In this manner we obtain

$$P_{\alpha_A, \alpha_B}(\Omega_A, \Omega_B; t_r, \tau) \propto \sum_{m, m', q, q'=-1}^1 \sum_{j, j', j'', j'''=1}^N e^{i\mathbf{k}_{32} \cdot \mathbf{R}_j} e^{i\mathbf{k}_{21} \cdot \mathbf{R}_{j'}} e^{-i\mathbf{k}_{21} \cdot \mathbf{R}_{j''}} e^{-i\mathbf{k}_{32} \cdot \mathbf{R}_{j'''}} [\mathbf{Q}_{m3}^*]_{\alpha_A} [\mathbf{Q}_{m'1}^*]_{\alpha_B} [\mathbf{Q}_{1q}]_{\alpha_B} [\mathbf{Q}_{q'3}]_{\alpha_A} \times \langle \sigma_{3m}^{(j)}(t_r) \sigma_{m'1}^{(j')}(t_r + \tau) \sigma_{1q}^{(j'')}(t_r + \tau) \sigma_{q'3}^{(j''')}(t_r) \rangle. \quad (\text{B55})$$

Using the quantum regression theorem [22] in connection with Eqs. (B6), we can obtain

$$\langle \sigma_{3m}^{(j)}(t_r) \sigma_{m'1}^{(j')}(t_r + \tau) \sigma_{1q}^{(j'')}(t_r + \tau) \sigma_{q'3}^{(j''')}(t_r) \rangle = \langle \sigma_{3m}^{(j)}(t_r) \sigma_{m'1}^{(j')}(t_r) \sigma_{1q}^{(j'')}(t_r) \sigma_{q'3}^{(j''')}(t_r) \rangle e^{-\Gamma_2 \tau} + \gamma_{j'j'', m'q} \frac{e^{-\Gamma_2 t_r} - e^{-\gamma_3 t_r}}{\gamma_3 - \Gamma_2} \langle \sigma_{3m}^{(j)}(t_r) \sigma_{31}^{(j)}(t_r) \sigma_{13}^{(j')}(t_r) \sigma_{q'3}^{(j''')}(t_r) \rangle. \quad (\text{B56})$$

For our initial conditions, the second term vanishes and the first contributes only if $j = j'$ and $j' = j''$. Explicitly,

$$\langle \sigma_{3m}^{(j)}(t_r) \sigma_{m'1}^{(j')}(t_r + \tau) \sigma_{1q}^{(j'')}(t_r + \tau) \sigma_{q'3}^{(j''')}(t_r) \rangle = \rho_{33}(0) e^{-\gamma_3 t} e^{-\Gamma_2 \tau} \delta(j, j', j'', j''') \delta(m, m') \delta(q, q') + \langle \sigma_{31}^{(j)}(0) \sigma_{13}^{(j')}(0) \rangle e^{-i\mathbf{k} \cdot \mathbf{R}_{j'}} e^{-\gamma_3 t} e^{-\Gamma_2 \tau} \delta(j, j') \delta(j'', j''') \delta(m, m') \delta(q, q'), \quad (\text{B57})$$

where the δ functions are equal to unity when all arguments are equal and vanish otherwise.

Equation (B57) is substituted into Eq. (B55), the summations over m, m', q, q' are carried out, and the summations over j, j', j'', j''' are converted to integrals using the prescription (B39), then we find that $P_{\alpha_A, \alpha_B}(\Omega_A, \Omega_B; t_r, \tau)$ is given by Eq. (43).

-
- [1] H. J. Kimble, A. Mezzacappa, and P. W. Milonni, *Phys. Rev. A* **31**, 3686 (1985).
- [2] For a review, see M. B. Plenio and P. L. Knight, *Rev. Mod. Phys.* **70**, 101 (1998).
- [3] A. Aspect, P. Grangier, and G. Roger, *Phys. Rev. Lett.* **47**, 460 (1981).
- [4] See, for example, M. Saffman, T. G. Walker, and K. Mølmer, *Rev. Mod. Phys.* **82**, 2313 (2010), and references therein; Y. O. Dudin and A. Kuzmich, *Science* **336**, 887 (2012); P. Schauß, M. Cheneau, M. Endres, T. Fukuhara, S. Hild, A. Omran, T. Pohl, C. Gross, S. Kuhr, and I. Bloch, *Nature (London)* **491**, 87 (2012); T. Jeong, J. Park, and H. S. Moon, *Phys. Rev. A* **100**, 033818 (2019).
- [5] See, for example, T. Chanelière, D. N. Matsukevich, S. D. Jenkins, T. A. B. Kennedy, M. S. Chapman, and A. Kuzmich, *Phys. Rev. Lett.* **96**, 093604 (2006); R. T. Willis, F. E. Becerra, L. A. Orozco, and S. L. Rolston, *Phys. Rev. A* **82**, 053842 (2010); G. K. Gulati, B. Srivathsan, B. Chng, A. Cerè, and C. Kurtsiefer, *New J. Phys.* **17**, 093034 (2015); Y.-S. Lee, S. M. Lee, H. Kim, and H. S. Moon, *Phys. Rev. A* **96**, 063832 (2017); T. Jeong and H. S. Moon, *Opt. Lett.* **45**, 2668 (2020).
- [6] S. D. Jenkins, D. N. Matsukevich, T. Chanelière, S.-Y. Lan, T. A. B. Kennedy, and A. Kuzmich, *J. Opt. Soc. Am. B* **24**, 316 (2007).
- [7] H. H. Jen, *Phys. Rev. A* **85**, 013835 (2012).
- [8] H. H. Jen, *Phys. Rev. A* **95**, 043840 (2017).
- [9] M. D. Lukin, M. Fleischhauer, R. Cote, L. M. Duan, D. Jaksch, J. I. Cirac, and P. Zoller, *Phys. Rev. Lett.* **87**, 037901 (2001).
- [10] For a review, see P. R. Berman and D. G. Steel, in *Handbook of Optics*, Vol. IV, 3rd ed., edited by M. Bass, G. Li, and E. van Stryland (McGraw-Hill, New York, 2010), pp. 11.1–11.34.
- [11] P. R. Berman, *Am. J. Phys.* **78**, 1323 (2010).
- [12] N. E. Rehler and J. H. Eberly, *Phys. Rev. A* **3**, 1735 (1971).
- [13] R. H. Dicke, *Phys. Rev.* **93**, 99 (1954).
- [14] M. J. Stephen, *J. Chem Phys.* **40**, 669 (1964).
- [15] D. A. Hutchinson and H. F. Hameka, *J. Chem Phys.* **41**, 2006 (1964).
- [16] R. H. Lehberg, *Phys. Rev. A* **2**, 889 (1970).
- [17] See, for example, A. A. Svidzinsky, J.-T. Chang, and M. O. Scully, *Phys. Rev. Lett.* **100**, 160504 (2008); A. A. Svidzinsky and J.-T. Chang, *Phys. Rev. A* **77**, 043833 (2008).
- [18] See, for example, R. Friedberg and J. T. Manassah, *Opt. Commun.* **281**, 3755 (2008); *Phys. Lett. A* **374**, 1648 (2010).
- [19] Y. Miroshnychenko, U. V. Poulsen, and K. Mølmer, *Phys. Rev. A* **87**, 023821 (2013).
- [20] This equation is valid only in the limit $k_{32}a > 10$, $k_{21}L > 10$, and $F_{32} \geq 1$. The more general result is given by Eq. (B52).
- [21] For $kL > 100$ the agreement gets worse because the Fresnel number is no longer greater than unity.
- [22] See, for example, C. Claude-Tannoudji, J. Dupont-Roc, and G. Gilbert, *Atom-Photon Interactions* (Wiley Interscience, New York, 1992), pp. 388–405.
- [23] P. R. Berman and V. S. Malinovsky, *Principles of Laser Spectroscopy and Quantum Optics* (Princeton University Press, Princeton, 2011), pp. 461–465.